3 Quark masses

Authors: T. Blum, A. Portelli, A. Ramos

Quark masses are fundamental parameters of the Standard Model. An accurate determination of these parameters is important for both phenomenological and theoretical applications. The bottom- and charm-quark masses, for instance, are important sources of parametric uncertainties in several Higgs decay modes. The up-, down- and strange-quark masses govern the amount of explicit chiral symmetry breaking in QCD. From a theoretical point of view, the values of quark masses provide information about the flavour structure of physics beyond the Standard Model. The Review of Particle Physics of the Particle Data Group contains a review of quark masses [1], which covers light as well as heavy flavours. Here we also consider light- and heavy-quark masses, but focus on lattice results and discuss them in more detail. We do not discuss the top quark, however, because it decays weakly before it can hadronize, and the nonperturbative QCD dynamics described by present day lattice simulations is not relevant. The lattice determination of light- (up, down, strange), charm- and bottom-quark masses is considered below in Secs. 3.1, 3.2, and 3.3, respectively.

Quark masses cannot be measured directly in experiment because quarks cannot be isolated, as they are confined inside hadrons. From a theoretical point of view, in QCD with N_f flavours, a precise definition of quark masses requires one to choose a particular renormalization scheme. This renormalization procedure introduces a renormalization scale μ, and quark masses depend on this renormalization scale according to the Renormalization Group (RG) equations. In mass-independent renormalization schemes the RG equations read

$$\mu \frac{\mathrm{d}\bar{m}_i(\mu)}{\mathrm{d}\mu} = \bar{m}_i(\mu)\tau(\bar{g})\,, \tag{20}$$

where the function $\tau(\bar{g})$ is the anomalous dimension, which depends only on the value of the strong coupling $\alpha_s = \bar{g}^2/(4\pi)$. Note that in QCD $\tau(\bar{g})$ is the same for all quark flavours. The anomalous dimension is scheme dependent, but its perturbative expansion

$$\tau(\bar{g}) \overset{\bar{g}\to 0}{\sim} -\bar{g}^2\left(d_0 + d_1\bar{g}^2 + \dots\right) \tag{21}$$

has a leading coefficient $d_0 = 8/(4\pi)^2$, which is scheme independent.[1] Equation (20), being a first order differential equation, can be solved exactly by using Eq. (21) as the boundary condition. The formal solution of the RG equation reads

$$M_i = \bar{m}_i(\mu)[2b_0\bar{g}^2(\mu)]^{-d_0/(2b_0)} \exp\left\{-\int_0^{\bar{g}(\mu)} \mathrm{d}x \left[\frac{\tau(x)}{\beta(x)} - \frac{d_0}{b_0 x}\right]\right\}\,, \tag{22}$$

where $b_0 = (11 - 2N_f/3)/(4\pi)^2$ is the universal leading perturbative coefficient in the expansion of the β-function, $\beta(\bar{g}) \equiv (1/4\pi)d\bar{g}^2/d\log\mu^2$, which governs the running of the strong coupling constant near the scale μ. The renormalization group invariant (RGI) quark masses M_i are formally integration constants of the RG Eq. (20). They are scale independent, and due to the universality of the coefficient d_0, they are also scheme independent. Moreover, they are nonperturbatively defined by Eq. (22). They only depend on the number of flavours N_f, making them a natural candidate to quote quark masses and compare determinations from

[1] We follow the conventions of Gasser and Leutwyler [2].

different lattice collaborations. Nevertheless, it is customary in the phenomenology community to use the $\overline{\text{MS}}$ scheme at a scale $\mu = 2$ GeV to compare different results for light-quark masses, and use a scale equal to its own mass for the charm and bottom quarks. In this review, we will quote the final averages of both quantities.

Results for quark masses are always quoted in the four-flavour theory. $N_f = 2+1$ results have to be converted to the four-flavour theory. Fortunately, the charm quark is heavy $(\Lambda_{\text{QCD}}/m_c)^2 < 1$, and this conversion can be performed in perturbation theory with negligible ($\sim 0.2\%$) perturbative uncertainties. Nonperturbative corrections in this matching are more difficult to estimate. Since these effects are suppressed by a factor of $1/N_{\text{c}}$, and a factor of the strong coupling at the scale of the charm mass, naive power counting arguments would suggest that the effects are $\sim 1\%$. In practice, numerical nonperturbative studies [3–5] have found this power counting argument to be an overestimate by one order of magnitude in the determination of simple hadronic quantities or the Λ-parameter. Moreover, lattice determinations do not show any significant deviation between the $N_f = 2{+}1$ and $N_f = 2{+}1{+}1$ simulations. For example, the difference in the final averages for the mass of the strange quark m_s between $N_f = 2{+}1$ and $N_f = 2{+}1{+}1$ determinations is about 1.3%, or about one standard deviation.

We quote all final averages at 2 GeV in the $\overline{\text{MS}}$ scheme and also the RGI values (in the four-flavour theory). We use the exact RG Eq. (22). Note that to use this equation we need the value of the strong coupling in the $\overline{\text{MS}}$ scheme at a scale $\mu = 2$ GeV. All our results are obtained from the RG equation in the $\overline{\text{MS}}$ scheme and the 5-loop beta function together with the value of the Λ-parameter in the four-flavour theory $\Lambda^{(4)}_{\overline{\text{MS}}} = 294(12)\,\text{MeV}$ obtained in this review (see Sec. 9). In the uncertainties of the RGI masses we separate the contributions from the determination of the quark masses and the propagation of the uncertainty of $\Lambda^{(4)}_{\overline{\text{MS}}}$. These are identified with the subscripts m and Λ, respectively.

Conceptually, all lattice determinations of quark masses contain three basic ingredients:

1. Tuning the lattice bare-quark masses to match the experimental values of some quantities. Pseudo-scalar meson masses provide the most common choice, since they have a strong dependence on the values of quark masses. In pure QCD with N_f quark flavours these values are not known, since the electromagnetic interactions affect the experimental values of meson masses. Therefore, pure QCD determinations use model/lattice information to determine the location of the physical point. This is discussed at length in Sec. 3.1.1.

2. Renormalization of the bare-quark masses. Bare-quark masses determined with the above-mentioned criteria have to be renormalized. Many of the latest determinations use some nonperturbatively defined scheme. One can also use perturbation theory to connect directly the values of the bare-quark masses to the values in the $\overline{\text{MS}}$ scheme at 2 GeV. Experience shows that 1-loop calculations are unreliable for the renormalization of quark masses: usually at least two loops are required to have trustworthy results.

3. If quark masses have been nonperturbatively renormalized, for example, to some MOM/SF scheme, the values in this scheme must be converted to the phenomenologically useful values in the $\overline{\text{MS}}$ scheme (or to the scheme/scale independent RGI masses). Either option requires the use of perturbation theory. The larger the energy scale of this matching with perturbation theory, the better, and many recent computations in MOM schemes do a nonperturbative running up to 3–4 GeV. Computations in the SF scheme allow

us to perform this running nonperturbatively over large energy scales and match with perturbation theory directly at the electro-weak scale ~ 100 GeV.

Note that many lattice determinations of quark masses make use of perturbation theory at a scale of a few GeV.

We mention that lattice-QCD calculations of the b-quark mass have an additional complication which is not present in the case of the charm and light quarks. At the lattice spacings currently used in numerical simulations the direct treatment of the b quark with the fermionic actions commonly used for light quarks is very challenging. Only two determinations of the b-quark mass use this approach, reaching the physical b-quark mass region at two lattice spacings with $aM \sim 1$. There are a few widely used approaches to treat the b quark on the lattice, which have been already discussed in the FLAG 13 review (see Sec. 8 of Ref. [6]). Those relevant for the determination of the b-quark mass will be briefly described in Sec. 3.3.

3.1 Masses of the light quarks

Light-quark masses are particularly difficult to determine because they are very small (for the up and down quarks) or small (for the strange quark) compared to typical hadronic scales. Thus, their impact on typical hadronic observables is minute, and it is difficult to isolate their contribution accurately.

Fortunately, the spontaneous breaking of $SU(3)_L \times SU(3)_R$ chiral symmetry provides observables which are particularly sensitive to the light-quark masses: the masses of the resulting Nambu-Goldstone bosons (NGB), i.e., pions, kaons, and eta. Indeed, the Gell-Mann-Oakes-Renner relation [7] predicts that the squared mass of a NGB is directly proportional to the sum of the masses of the quark and antiquark which compose it, up to higher-order mass corrections. Moreover, because these NGBs are light, and are composed of only two valence particles, their masses have a particularly clean statistical signal in lattice-QCD calculations. In addition, the experimental uncertainties on these meson masses are negligible. Thus, in lattice calculations, light-quark masses are typically obtained by renormalizing the input quark mass and tuning them to reproduce NGB masses, as described above.

3.1.1 The physical point and isospin symmetry

As mentioned in Sec. 2.1, the present review relies on the hypothesis that, at low energies, the Lagrangian $\mathcal{L}_{\rm QCD} + \mathcal{L}_{\rm QED}$ describes nature to a high degree of precision. However, most of the results presented below are obtained in pure QCD calculations, which do not include QED. Quite generally, when comparing QCD calculations with experiment, radiative corrections need to be applied. In pure QCD simulations, where the parameters are fixed in terms of the masses of some of the hadrons, the electromagnetic contributions to these masses must be discussed. How the matching is done is generally ambiguous because it relies on the unphysical separation of QCD and QED contributions. In this section, and in the following, we discuss this issue in detail. A related discussion, in the context of scale setting, is given in Sec. 11.3. Of course, once QED is included in lattice calculations, the subtraction of electromagnetic contributions is no longer necessary.

Let us start from the unambiguous case of QCD+QED. As explained in the introduction of this section, the physical quark masses are the parameters of the Lagrangian such that a given set of experimentally measured, dimensionful hadronic quantities are reproduced by the theory. Many choices are possible for these quantities, but in practice many lattice groups use pseudoscalar meson masses, as they are easily and precisely obtained both by experiment, and through lattice simulations. For example, in the four-flavour case, one can solve the system

$$M_{\pi^+}(m_u, m_d, m_s, m_c, \alpha) = M_{\pi^+}^{\text{exp.}}, \quad (23)$$

$$M_{K^+}(m_u, m_d, m_s, m_c, \alpha) = M_{K^+}^{\text{exp.}}, \quad (24)$$

$$M_{K^0}(m_u, m_d, m_s, m_c, \alpha) = M_{K^0}^{\text{exp.}}, \quad (25)$$

$$M_{D^0}(m_u, m_d, m_s, m_c, \alpha) = M_{D^0}^{\text{exp.}}, \quad (26)$$

where we assumed that

- all the equations are in the continuum and infinite-volume limits;
- the overall scale has been set to its physical value, generally through some lattice-scale setting procedure involving a fifth dimensionful input (see the discussion in Sec. 11.3);
- the quark masses m_q are assumed to be renormalized from the bare, lattice ones in some given continuum renormalization scheme;
- $\alpha = \frac{e^2}{4\pi}$ is the fine-structure constant expressed as function of the positron charge e, generally set to the Thomson limit $\alpha = 0.007297352\ldots$ [1];
- the mass $M_h(m_u, m_d, m_s, m_c, \alpha)$ of the meson h is a function of the quark masses and α. The functional dependence is generally obtained by choosing an appropriate parameterization and performing a global fit to the lattice data;
- the superscript exp. indicates that the mass is an experimental input, lattice groups use in general the values in the Particle Data Group review [1].

However, ambiguities arise with simulations of QCD only. In that case, there is no experimentally measurable quantity that emerges from the strong interaction only. The missing QED contribution is tightly related to isospin-symmetry breaking effects. Isospin symmetry is explicitly broken by the differences between the up- and down-quark masses $\delta m = m_u - m_d$, and electric charges $\delta Q = Q_u - Q_d$. These effects are, respectively, of order $\mathcal{O}(\delta m/\Lambda_{\text{QCD}})$ and $\mathcal{O}(\alpha)$, and are expected to be $\mathcal{O}(1\%)$ of a typical isospin-symmetric hadronic quantity. Strong and electromagnetic isospin-breaking effects are of the same order and therefore cannot, in principle, be evaluated separately without introducing strong ambiguities. Because these effects are small, they can be treated as a perturbation,

$$X(m_u, m_d, m_s, m_c, \alpha) = \bar{X}(m_{ud}, m_s, m_c) + \delta m A_X(m_{ud}, m_s, m_c) + \alpha B_X(m_{ud}, m_s, m_c), \quad (27)$$

for a given hadronic quantity X, where $m_{ud} = \frac{1}{2}(m_u + m_d)$ is the average light-quark mass. There are several things to notice here. Firstly, the neglected higher-order $\mathcal{O}(\delta m^2, \alpha\delta m, \alpha^2)$ corrections are expected to be $\mathcal{O}(10^{-4})$ relatively to X, which at the moment is way beyond the relative statistical accuracy that can be delivered by a lattice calculation. Secondly, this is not strictly speaking an expansion around the isospin-symmetric point, the electromagnetic interaction has also symmetric contributions. From this last expression the previous statements about ambiguities become clearer. Indeed, the only unambiguous prediction one can perform is to solve Eqs. (23)–(26) and use the resulting parameters to obtain a prediction for X, which is represented by the left-hand side of Eq. (27). This prediction will be the sum of the QCD isospin-symmetric part $\bar{X}$, the strong isospin-breaking effects $X^{SU(2)} = \delta m A_X$, and the electromagnetic effects $X^{\gamma} = \alpha B_X$. Obtaining any of these terms individually requires extra, unphysical conditions to perform the separation. To be consistent with previous editions of FLAG, we also define $\hat{X} = \bar{X} + X^{SU(2)}$ to be the $\alpha \to 0$ limit of X.

With pure QCD simulations, one typically solves Eqs. (23)–(26) by equating the QCD isospin-symmetric part of a hadron mass $\bar{M}_h$, result of the simulations, with its experimental value $M_h^{\mathrm{exp.}}$. This will result in an $\mathcal{O}(\delta m, \alpha)$ mis-tuning of the theory parameters which will propagate as an error on predicted quantities. Because of this, in general, one cannot predict hadronic quantities with a relative accuracy higher than $\mathcal{O}(1\%)$ from pure QCD simulations, independently on how the target X is sensitive to isospin-breaking effects. If one performs a complete lattice prediction of the physical value of X, it can be of phenomenological interest to define in some way $\bar{X}$, $X^{SU(2)}$, and X^{γ}. If we keep m_{ud}, m_s and m_c at their physical values in physical units, for a given renormalization scheme and scale, then these three quantities can be extracted by setting successively and simultaneously α and δm to 0. This is where the ambiguity lies: in general the $\delta m = 0$ point will depend on the renormalization scheme used for the quark masses. In the next section, we give more details on that particular aspect and discuss the order of scheme ambiguities.

3.1.2 Ambiguities in the separation of isospin-breaking contributions

In this section, we discuss the ambiguities that arise in the individual determination of the QED contribution X^{γ} and the strong-isospin correction $X^{SU(2)}$ defined in the previous section. Throughout this section, we assume that the isospin-symmetric quark masses m_{ud}, m_s and m_c are always kept fixed in physical units to the values they take at the QCD+QED physical point in some given renormalization scheme. Let us assume that both up and down masses have been renormalized in an identical mass-independent scheme which depends on some energy scale μ. We also assume that the renormalization procedure respects chiral symmetry so that quark masses renormalize multiplicatively. The renormalization constants of the quark masses are identical for $\alpha = 0$ and therefore the renormalized mass of a quark has the general form

$$m_q(\mu) = Z_m(\mu)[1 + \alpha Q_{\mathrm{tot.}}^2 \delta_Z^{(0)}(\mu) + \alpha Q_{\mathrm{tot.}} Q_q \delta_Z^{(1)}(\mu) + \alpha Q_q^2 \delta_Z^{(2)}(\mu)] m_{q,0}\,, \tag{28}$$

up to $\mathcal{O}(\alpha^2)$ corrections, where $m_{q,0}$ is the bare-quark mass, $Q_{\mathrm{tot.}}$ and $Q_{\mathrm{tot.}}^2$ are the sum of all quark charges and squared charges, respectively, and Q_q is the quark charge, all in units of in units of the positron charge e. Throughout this section, a subscript ud generally denotes the average between up and down quantities and δ the difference between the up and the down quantities. The source of the ambiguities described in the previous section is the mixing of the isospin-symmetric mass m_{ud} and the difference δm through renormalization. Using Eq. (28) one can make this mixing explicit at leading order in α:

$$\begin{pmatrix} m_{ud}(\mu) \\ \delta m(\mu) \end{pmatrix} = Z_m(\mu)[1 + \alpha Q_{\mathrm{tot.}}^2 \delta_Z^{(0)}(\mu) + \alpha M^{(1)}(\mu) + \alpha M^{(2)}(\mu)] \begin{pmatrix} m_{ud,0} \\ \delta m_0 \end{pmatrix} \tag{29}$$

with the mixing matrices

$$M^{(1)}(\mu) = \delta_Z^{(1)}(\mu) Q_{\mathrm{tot.}} \begin{pmatrix} Q_{ud} & \frac{1}{4}\delta Q \\ \delta Q & Q_{ud} \end{pmatrix} \qquad \text{and} \qquad M^{(2)}(\mu) = \delta_Z^{(2)}(\mu) \begin{pmatrix} Q_{ud}^2 & \frac{1}{4}\delta Q^2 \\ \delta Q^2 & Q_{ud}^2 \end{pmatrix}\,, \tag{30}$$

where $Q_{ud} = \frac{1}{2}(Q_u + Q_d)$ and $\delta Q = Q_u - Q_d$ are the average and difference of the up and down charges, and similarly $Q_{ud}^2 = \frac{1}{2}(Q_u^2 + Q_d^2)$ and $\delta Q^2 = Q_u^2 - Q_d^2$ for the squared charges.

Now let us assume that for the purpose of determining the different components in Eq. (27), one starts by tuning the bare masses to obtain equal up and down masses, for some small coupling α_0 at some scale μ_0, i.e., $\delta m(\mu_0) = 0$. At this specific point, one can extract the pure QCD, and the QED corrections to a given quantity X by studying the slope of α in Eq. (27). From these quantities the strong-isospin contribution can then readily be extracted using a nonzero value of $\delta m(\mu_0)$. However, if now the procedure is repeated at another coupling α and scale μ with the same bare masses, it appears from Eq. (29) that $\delta m(\mu) \neq 0$. More explicitly,

$$\delta m(\mu) = m_{ud}(\mu_0)\frac{Z_m(\mu)}{Z_m(\mu_0)}[\alpha\Delta_Z(\mu) - \alpha_0\Delta_Z(\mu_0)]\,, \tag{31}$$

with

$$\Delta_Z(\mu) = Q_{\rm tot.}\delta Q\delta_Z^{(1)}(\mu) + \delta Q^2\delta_Z^{(2)}(\mu)\,, \tag{32}$$

up to higher-order corrections in α and α_0. In other words, the definitions of $\bar{X}$, $X^{SU(2)}$, and X^γ depend on the renormalization scale at which the separation was made. This dependence, of course, has to cancel in the physical sum X. One can notice that at no point did we mention the renormalization of α itself, which, in principle, introduces similar ambiguities. However, the corrections coming from the running of α are $\mathcal{O}(\alpha^2)$ relatively to X, which, as justified above, can be safely neglected. Finally, important information is provided by Eq. (31): the scale ambiguities are $\mathcal{O}(\alpha m_{ud})$. For physical quark masses, one generally has $m_{ud} \simeq \delta m$. So by using this approximation in the first-order expansion Eq. (27), it is actually possible to define unambiguously the components of X up to second-order isospin-breaking corrections. Therefore, in the rest of this review, we will not keep track of the ambiguities in determining pure QCD or QED quantities. However, in the context of lattice simulations, it is crucial to notice that $m_{ud} \simeq \delta m$ is only accurate *at the physical point*. In simulations at larger-than-physical pion masses, scheme ambiguities in the separation of QCD and QED contributions are generally large. Once more, the argument made here assumes that the isospin-symmetric quark masses m_{ud}, m_s, and m_c are kept fixed to their physical value in a given scheme while varying α. Outside of this assumption there is an additional isospin-symmetric $O(\alpha m_q)$ ambiguity between $\bar{X}$ and X^γ.

Such separation in lattice QCD+QED simulation results appeared for the first time in RBC 07 [8] and Blum 10 [9], where the scheme was implicitly defined around the χPT expansion. In that setup, the $\delta m(\mu_0) = 0$ point is defined in pure QCD, i.e., $\alpha_0 = 0$ in the previous discussion. The QCD part of the kaon-mass splitting from the first FLAG review [10] is used as an input in RM123 11 [11], which focuses on QCD isospin corrections only. It therefore inherits from the convention that was chosen there, which is also to set $\delta m(\mu_0) = 0$ at zero QED coupling. The same convention was used in the follow-up works RM123 13 [12] and RM123 17 [13]. The BMW collaboration was the first to introduce a purely hadronic scheme in its electro-quenched study of the baryon octet mass splittings [14]. In this work, the quark mass difference $\delta m(\mu)$ is swapped with the mass splitting ΔM^2 between the connected $\bar{u}u$ and $\bar{d}d$ pseudoscalar masses. Although unphysical, this quantity is proportional [15] to $\delta m(\mu)$ up to $\mathcal{O}(\alpha m_{ud})$ chiral corrections. In this scheme, the quark masses are assumed to be equal at $\Delta M^2 = 0$, and the $\mathcal{O}(\alpha m_{ud})$ corrections to this statement are analogous to the scale ambiguities mentioned previously. The same scheme was used for the determination of light-quark masses in BMW 16 [16] and in the recent BMW prediction of the leading hadronic contribution to the muon magnetic moment [17]. The BMW collaboration used a different hadronic scheme for its determination of the nucleon-mass splitting in BMW 14 [18] using full

QCD+QED simulations. In this work, the $\delta m = 0$ point was fixed by imposing the baryon splitting $M_{\Sigma^+} - M_{\Sigma^-}$ to cancel. This scheme is quite different from the other ones presented here, in the sense that its intrinsic ambiguity is not $\mathcal{O}(\alpha m_{ud})$. What motivates this choice here is that $M_{\Sigma^+} - M_{\Sigma^-} = 0$ in the limit where these baryons are point particles, so the scheme ambiguity is suppressed by the compositeness of the Σ baryons. This may sound like a more difficult ambiguity to quantify, but this scheme has the advantage of being defined purely by measurable quantities. Moreover, it has been demonstrated numerically in BMW 14 [18] that, within the uncertainties of this study, the $M_{\Sigma^+} - M_{\Sigma^-} = 0$ scheme is equivalent to the $\Delta M^2 = 0$ one, explicitly $M_{\Sigma^+} - M_{\Sigma^-} = -0.18(12)(6)\,\mathrm{MeV}$ at $\Delta M^2 = 0$. The calculation QCDSF/UKQCD 15 [19] uses a "Dashen scheme," where quark masses are tuned such that flavour-diagonal mesons have equal masses in QCD and QCD+QED. Although not explicitly mentioned by the authors of the paper, this scheme is simply a reformulation of the $\Delta M^2 = 0$ scheme mentioned previously. Finally, MILC 18 [20] also used the $\Delta M^2 = 0$ scheme and noticed its connection to the "Dashen scheme" from QCDSF/UKQCD 15.

Before the previous edition of this review, the contributions $\bar{X}$, $X^{SU(2)}$, and X^{γ} were given for pion and kaon masses based on phenomenological information. Considerable progress has been achieved by the lattice community to include isospin-breaking effects in calculations, and it is now possible to determine these quantities precisely directly from a lattice calculation. However, these quantities generally appear as intermediate products of a lattice analysis, and are rarely directly communicated in publications. These quantities, although unphysical, have a phenomenological interest, and we encourage the authors of future calculations to quote them explicitly.

3.1.3 Inclusion of electromagnetic effects in lattice-QCD simulations

Electromagnetism on a lattice can be formulated using a naive discretization of the Maxwell action $S[A_\mu] = \frac{1}{4}\int d^4x \sum_{\mu,\nu}[\partial_\mu A_\nu(x) - \partial_\nu A_\mu(x)]^2$. Even in its noncompact form, the action remains gauge invariant. This is not the case for non-Abelian theories for which one uses the traditional compact Wilson gauge action (or an improved version of it). Compact actions for QED feature spurious photon-photon interactions which vanish only in the continuum limit. This is one of the main reason why the noncompact action is the most popular so far. It was used in all the calculations presented in this review. Gauge-fixing is necessary for noncompact actions because of the usual infinite measure of equivalent gauge orbits which contribute to the path integral. It was shown [21, 22] that gauge-fixing is not necessary with compact actions, including in the construction of interpolating operators for charged states.

Although discretization is straightforward, simulating QED in a finite volume is more challenging. Indeed, the long range nature of the interaction suggests that important finite-size effects have to be expected. In the case of periodic boundary conditions, the situation is even more critical: a naive implementation of the theory features an isolated zero-mode singularity in the photon propagator. It was first proposed in [23] to fix the global zero-mode of the photon field $A_\mu(x)$ in order to remove it from the dynamics. This modified theory is generally named $\mathrm{QED_{TL}}$. Although this procedure regularizes the theory and has the right classical infinite-volume limit, it is nonlocal because of the zero-mode fixing. As first discussed in [18], the nonlocality in time of $\mathrm{QED_{TL}}$ prevents the existence of a transfer matrix, and therefore a quantum-mechanical interpretation of the theory. Another prescription named $\mathrm{QED_L}$, proposed in [24], is to remove the zero-mode of $A_\mu(x)$ independently for each time slice. This theory, although still nonlocal in space, is local in time and has a well-defined transfer matrix. Whether these nonlocalities constitute an issue to extract infinite-volume physics from lattice-QCD+QED$_\mathrm{L}$ simulations is, at the time of this review, still an open question. However, it is known through analytical calculations of electromagnetic finite-size effects at $O(\alpha)$ in hadron masses [12, 18, 24–28], meson leptonic decays [27], and the hadronic vacuum polarization [29] that QED$_\mathrm{L}$ does not suffer from a problematic (e.g., UV divergent) coupling of short- and long-distance physics due to its nonlocality. Another strategy, first proposed in [30] and used by the QCDSF collaboration, is to bound the zero-mode fluctuations to a finite range. Although more minimal, it is still a nonlocal modification of the theory and so far finite-size effects for this scheme have not been investigated. More recently, two proposals for local formulations of finite-volume QED emerged. The first one described in [31] proposes to use massive photons to regulate zero-mode singularities, at the price of (softly) breaking gauge invariance. The second one presented in [22], based on earlier works [32, 33], avoids the zero-mode issue by using anti-periodic boundary conditions for $A_\mu(x)$. In this approach, gauge invariance requires the fermion field to undergo a charge conjugation transformation over a period, breaking electric charge conservation. These local approaches have the potential to constitute cleaner approaches to finite-volume QED. All the calculations presented in this review used QED$_\mathrm{L}$ or QED$_\mathrm{TL}$, with the exception of QCDSF.

Once a finite-volume theory for QED is specified, there are various ways to compute QED effects themselves on a given hadronic quantity. The most direct approach, first used in [23], is to include QED directly in the lattice simulations and assemble correlation functions from charged quark propagators. Another approach proposed in [12], is to exploit the perturbative nature of QED, and compute the leading-order corrections directly in pure QCD as matrix elements of the electromagnetic current. Both approaches have their advantages and disadvantages and as shown in [13], are not mutually exclusive. A critical comparative study can be found in [34].

Finally, most of the calculations presented here made the choice of computing electromagnetic corrections in the electro-quenched approximation. In this limit, one assumes that only valence quarks are charged, which is equivalent to neglecting QED corrections to the fermionic determinant. This approximation reduces dramatically the cost of lattice-QCD+QED calculations since it allows the reuse of previously generated QCD configurations. If QED is introduced pertubatively through current insertions, the electro-quenched approximation avoids computing disconnected contributions coming from the electromagnetic current in the vacuum, which are generally challenging to determine precisely. The electromagnetic contributions from sea quarks to hadron-mass splittings are known to be flavour-$SU(3)$ and large-N_c suppressed, thus electro-quenched simulations are expected to have an $O(10\%)$ accuracy for the leading electromagnetic effects. This suppression is in principle rather weak and results obtained from electro-quenched simulations might feature uncontrolled systematic errors. For this reason, the use of the electro-quenched approximation constitutes the difference between ★ and ○ in the FLAG criterion for the inclusion of isospin-breaking effects.

3.1.4 Lattice determination of m_s and m_{ud}

We now turn to a review of the lattice calculations of the light-quark masses and begin with m_s, the isospin-averaged up- and down-quark mass m_{ud}, and their ratio. Most groups quote only m_{ud}, not the individual up- and down-quark masses. We then discuss the ratio m_u/m_d and the individual determinations of m_u and m_d.

Quark masses have been calculated on the lattice since the mid-nineties. However, early calculations were performed in the quenched approximation, leading to unquantifiable systematics. Thus, in the following, we only review modern, unquenched calculations, which include the effects of light sea quarks.

Tables 6 and 7 list the results of $N_f = 2 + 1$ and $N_f = 2 + 1 + 1$ lattice calculations of m_s and m_{ud}. These results are given in the $\overline{\mathrm{MS}}$ scheme at 2 GeV, which is standard nowadays, though some groups are starting to quote results at higher scales (e.g., Ref. [35]). The tables also show the colour coding of the calculations leading to these results. As indicated earlier in this review, we treat calculations with different numbers, N_f, of dynamical quarks separately.

$N_f = 2 + 1$ lattice calculations

We turn now to $N_f = 2 + 1$ calculations. These and the corresponding results for m_{ud} and m_s are summarized in Tab. 6. Given the very high precision of a number of the results, with total errors on the order of 1%, it is important to consider the effects neglected in these calculations. Isospin-breaking and electromagnetic effects are small on m_{ud} and m_s, and have been approximately accounted for in the calculations that will be retained for our averages. We have already commented that the effect of the omission of the charm quark in the sea is expected to be small, below our current precision, and we do not add any additional uncertainty due to these effects in the final averages.

The only new computation since the previous FLAG edition is the determination of light-quark masses by the ALPHA collaboration [36]. This work uses nonperturbatively $\mathcal{O}(a)$ improved Wilson fermions (a subset of the CLS ensembles [61]). The renormalization is performed nonperturbatively in the SF scheme from 200 MeV up to the electroweak scale ~ 100 GeV [62]. This nonperturbative running over such large energy scales avoids any use of perturbation theory at low energy scales, but adds a cost in terms of uncertainty: the running alone propagates to $\approx 1\%$ of the error in quark masses. This turns out to be one of the dominant pieces of uncertainty for the case of m_s. On the other hand, for the case of m_{ud}, the uncertainty is dominated by the chiral extrapolations. The ensembles used include four values of the lattice spacing below 0.09 fm, which qualifies for a ★ in the continuum extrapolation, and pion masses down to 200 MeV. This value lies just at the boundary of the ★ rating, but since the chiral extrapolation is a substantial source of systematic uncertainty, we opted to rate the work with a ○. In any case, this work enters in the average and their results show a reasonable agreement with the FLAG average.

We now comment in some detail on previous works that also contribute to the averages.

RBC/UKQCD 14 [38] significantly improves on their RBC/UKQCD 12B [35] work by adding three new domain wall fermion simulations to three used previously. Two of the new simulations are performed at essentially physical pion masses ($M_\pi \simeq 139\,\mathrm{MeV}$) on lattices of about 5.4 fm in size and with lattice spacings of 0.114 fm and 0.084 fm. It is complemented by a third simulation with $M_\pi \simeq 371\,\mathrm{MeV}$, $a \simeq 0.063$ fm and a rather small $L \simeq 2.0\,\mathrm{fm}$. Altogether, this gives them six simulations with six unitary ($m_{\mathrm{sea}} = m_{\mathrm{val}}$) M_π's in the range of 139 to 371 MeV, and effectively three lattice spacings from 0.063 to 0.114 fm. They perform a combined global continuum and chiral fit to all of their results for the π and K masses and decay constants, the Ω baryon mass and two Wilson-flow parameters. Quark masses in these fits are renormalized and run nonperturbatively in the RI-SMOM scheme. This is done by computing the relevant renormalization constant for a reference ensemble, and determining those for other simulations relative to it by adding appropriate parameters in the global fit. This calculation passes all of our selection criteria.

$N_f = 2+1$ MILC results for light-quark masses go back to 2004 [55, 56]. They use rooted staggered fermions. By 2009 their simulations covered an impressive range of parameter space, with lattice spacings going down to 0.045 fm, and valence-pion masses down to approximately 180 MeV [49]. The most recent MILC $N_f = 2+1$ results, i.e., MILC 10A [44] and MILC 09A [49], feature large statistics and 2-loop renormalization. Since these data sets subsume those of their previous calculations, these latest results are the only ones that need to be kept in any world average.

The BMW 10A, 10B [41, 42] calculation still satisfies our stricter selection criteria. They reach the physical up- and down-quark mass by *interpolation* instead of by extrapolation. Moreover, their calculation was performed at five lattice spacings ranging from 0.054 to 0.116 fm, with full nonperturbative renormalization and running and in volumes of up to $(6\text{ fm})^3$, guaranteeing that the continuum limit, renormalization, and infinite-volume extrapolation are controlled. It does neglect, however, isospin-breaking effects, which are small on the scale of their error bars.

Finally, we come to another calculation which satisfies our selection criteria, HPQCD 10 [45]. It updates the staggered-fermions calculation of HPQCD 09A [48]. In these papers, the renormalized mass of the strange quark is obtained by combining the result of a precise calculation of the renormalized charm-quark mass, m_c, with the result of a calculation of the quark-mass ratio, m_c/m_s. As described in Ref. [60] and in Sec. 3.2, HPQCD determines m_c by fitting Euclidean-time moments of the $\bar{c}c$ pseudoscalar density two-point functions, obtained numerically in lattice QCD, to fourth-order, continuum perturbative expressions. These moments are normalized and chosen so as to require no renormalization with staggered fermions. Since m_c/m_s requires no renormalization either, HPQCD's approach displaces the problem of lattice renormalization in the computation of m_s to one of computing continuum perturbative expressions for the moments. To calculate m_{ud} HPQCD 10 [45] use the MILC 09 determination of the quark-mass ratio m_s/m_{ud} [50].

HPQCD 09A [48] obtains $m_c/m_s = 11.85(16)$ [48] fully nonperturbatively, with a precision slightly larger than 1%. HPQCD 10's determination of the charm-quark mass, $m_c(m_c) = 1.268(6)$,[2] is even more precise, achieving an accuracy better than 0.5%.

This discussion leaves us with five results for our final average for m_s: ALPHA 19 [36], MILC 09A [49], BMW 10A, 10B [41, 42], HPQCD 10 [45] and RBC/UKQCD 14 [38]. Assuming that the result from HPQCD 10 is 100% correlated with that of MILC 09A, as it is based on a subset of the MILC 09A configurations, we find $m_s = 92.2(1.1)$ MeV with a χ^2/dof $= 1.65$.

For the light-quark mass m_{ud}, the results satisfying our criteria are ALPHA 19, RBC/UKQCD 14B, BMW 10A, 10B, HPQCD 10, and MILC 10A. For the error, we include the same 100% correlation between statistical errors for the latter two as for the strange case, resulting in the following (at scale 2 GeV in the $\overline{\text{MS}}$ scheme, and χ^2/dof=1.4),

$$N_f = 2+1: \qquad \begin{aligned} m_{ud} &= 3.381(40)\text{ MeV} \qquad &&\text{Refs. [36, 38, 41, 42, 44, 45]},\\ m_s &= 92.2(1.0)\text{ MeV} \qquad &&\text{Refs. [36, 38, 41, 42, 45, 49]}, \end{aligned} \tag{33}$$

and the RGI values

$$N_f = 2+1: \qquad \begin{aligned} M_{ud}^{\text{RGI}} &= 4.695(56)_m(54)_\Lambda\text{ MeV} \qquad &&\text{Refs. [36, 38, 41, 42, 44, 45]},\\ M_s^{\text{RGI}} &= 128.1(1.4)_m(1.5)_\Lambda\text{ MeV} \qquad &&\text{Refs. [36, 38, 41, 42, 45, 49]}. \end{aligned} \tag{34}$$

[2] To obtain this number, we have used the conversion from $\mu = 3$ GeV to m_c given in Ref. [60].

$N_f = 2+1+1$ lattice calculations

Since the previous review a new computation of m_s, m_{ud} has appeared, ETM 21A [63]. Using twisted-mass fermions with an added clover-term to suppress $\mathcal{O}(a^2)$ effects between the neutral and charged pions, this work represents a significant improvement over ETM 14 [64]. Renormalization is performed nonperturbatively in the RI-MOM scheme. Their ensembles comprise three lattice spacings (0.095, 0.082, and 0.069 fm), two volumes for the finest lattice spacings with pion masses reaching down to the physical point in the two finest lattices allowing a controlled chiral extrapolation. Their volumes are large, with $m_\pi L$ between four and five. These characteristics of their ensembles pass the most stringent FLAG criteria in all categories. This work extracts quark masses from two different quantities, one based on the meson spectrum and the other based on the baryon spectrum. Results obtained with these two methods agree within errors. The latter agrees well with the FLAG average while the former is high in comparison (there is good agreement with their previous results, ETM 14 [64]). Since ETM 21A was not published by the FLAG deadline, it is not included in the averages.

There are three other works that enter in light-quark mass averages: FNAL/MILC/TUMQCD 18 [65] (which contributes both to the average of m_{ud} and m_s), and the m_{ud} determinations in HPQCD 18 [66] and HPQCD 14A [67].

While the results of HPQCD 14A and HPQCD 18 agree well (using different methods), there are several tensions in the determination of m_s. The most significant discrepancy is between ETM 21A and the FLAG average. But also two recent and very precise determinations (HPQCD 18 and FNAL/MILC/TUMQCD 18) show a tension. Overall there is a rough agreement between the different determinations with $\chi^2/\mathrm{dof} = 1.7$ (that we apply to our average according to the standard FLAG averaging procedure). In the case of m_{ud} on the other hand only two works contribute to the average: ETM 14 and FNAL/MILC/TUMQCD 18. They disagree, with the FNAL/MILC/TUMQCD 18 value basically matching the $N_f = 2+1$ result. The large $\chi^2/\mathrm{dof} \approx 1.7$ increases significantly the error of the average. These large values of the χ^2 are difficult to understand in terms of a statistical fluctuation. On the other hand the $N_f = 2+1$ and $N_f = 2+1+1$ averages show a good agreement, which increases our confidence in the averages quoted below.

The $N_f = 2+1+1$ results are summarized in Tab. 7. Note that the results of Ref. [67] are reported as $m_s(2\,\mathrm{GeV}; N_f = 3)$ and those of Ref. [64] as $m_{ud(s)}(2\,\mathrm{GeV}; N_f = 4)$. We convert the former to $N_f = 4$ and obtain $m_s(2\,\mathrm{GeV}; N_f = 4) = 93.7(8)\mathrm{MeV}$. The average of FNAL/MILC/TUMQCD 18, HPQCD 18, ETM 14 and HPQCD 14A is 93.43(70)MeV with $\chi^2/\mathrm{dof} = 1.7$. For the light-quark average we use ETM 14 and FNAL/MILC/TUMQCD 18 with an average 3.410(43)MeV and a $\chi^2/\mathrm{dof} = 1.7$. We note these χ^2 values are large. For the case of the light-quark masses this is mostly due to ETM 14 masses lying significantly above the rest, but in the case of m_s there is also some tension between the recent and very precise results of HPQCD 18 and FNAL/MILC/TUMQCD 18. Also note that the 2+1-flavour values are consistent with the four-flavour ones, so in all cases we have decided to simply quote averages according to FLAG rules, including stretching factors for the errors based on χ^2 values of our fits:

$$N_f = 2+1+1: \qquad \begin{aligned} m_{ud} &= 3.410(43)\ \mathrm{MeV} &&\text{Refs. [64, 65]},\\ m_s &= 93.40(57)\ \mathrm{MeV} &&\text{Refs. [64–67]}, \end{aligned} \tag{35}$$

and the RGI values

$$N_f = 2+1+1: \qquad \begin{aligned} M_{ud}^{\rm RGI} &= 4.736(60)_m(55)_\Lambda \text{ MeV} \qquad && \text{Refs. [64, 65]}, \\ M_s^{\rm RGI} &= 129.7(0.8)_m(1.5)_\Lambda \text{ MeV} \qquad && \text{Refs. [64–67]}. \end{aligned} \tag{36}$$

In Figs. 1 and 2 the lattice results listed in Tabs. 6 and 7 and the FLAG averages obtained at each value of N_f are presented and compared with various phenomenological results.

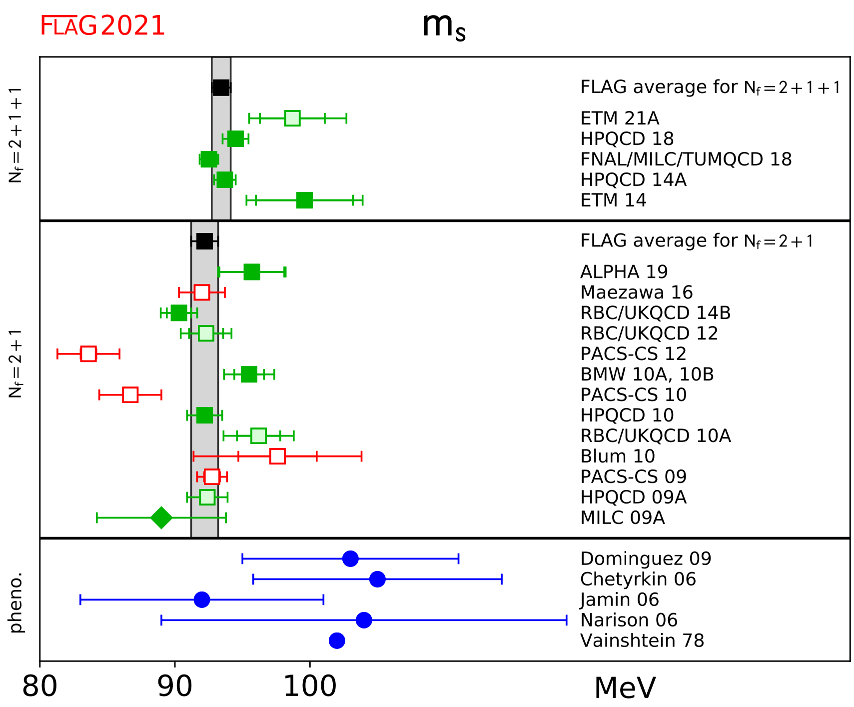

Figure 1: $\overline{\rm MS}$ mass of the strange quark (at 2 GeV scale) in MeV. The upper two panels show the lattice results listed in Tabs. 6 and 7, while the bottom panel collects sum rule results [68–72]. Diamonds and squares represent results based on perturbative and nonperturbative renormalization, respectively. The black squares and the grey bands represent our averages (33) and (35). The significance of the colours is explained in Sec. 2.

3.1.5 Lattice determinations of m_s/m_{ud}

The lattice results for m_s/m_{ud} are summarized in Tab. 8. In the ratio m_s/m_{ud}, one of the sources of systematic error—the uncertainties in the renormalization factors—drops out. Also other systematic effects (like the effect of the scale setting) are reduced in these ratios. This might explain that despite the discrepancies that are present in the individual quark mass determinations, the ratios show an overall very good agreement.

$N_f = 2+1$ *lattice calculations*

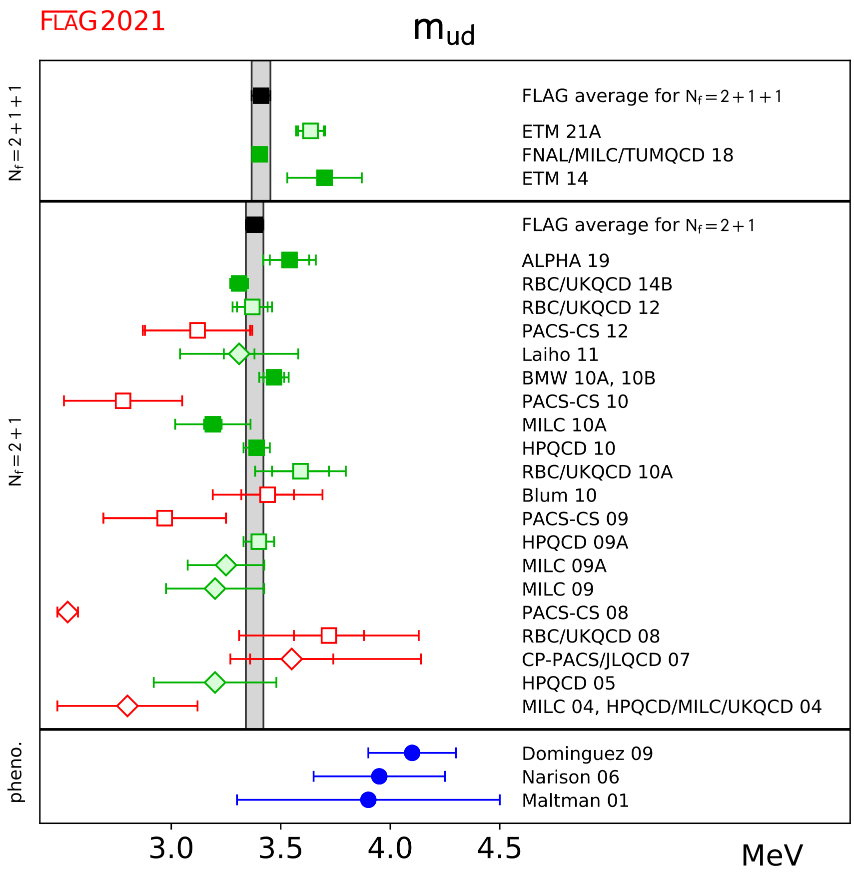

Figure 2: Mean mass of the two lightest quarks, $m_{ud} = \frac{1}{2}(m_u + m_d)$. The bottom panel shows results based on sum rules [68, 71, 73] (for more details see Fig. 1).

ALPHA 19 [36], discussed already, is the only new result for this section. The other works contributing to this average are RBC/UKQCD 14B, which replaces RBC/UKQCD 12 (see Sec. 3.1.4), and the results of MILC 09A and BMW 10A, 10B.

The results show very good agreement with a $\chi^2/\mathrm{dof} = 0.14$. The final uncertainty ($\approx 0.5\%$) is smaller than the ones of the quark masses themselves. At this level of precision, the uncertainties in the electromagnetic and strong isospin-breaking corrections might not be completely negligible. Nevertheless, we decided not to add any uncertainty associated with this effect. The main reason is that most recent determinations try to estimate this uncertainty themselves and found an effect smaller than naive power counting estimates (see $N_f = 2 + 1 + 1$ section),

$$N_f = 2+1: \qquad m_s/m_{ud} = 27.42\ (12) \qquad \text{Refs. [36, 38, 41, 42, 49]}. \tag{37}$$

$N_f = 2 + 1 + 1$ lattice calculations

For $N_f = 2+1+1$ there are three results, MILC 17 [74], ETM 14 [64] and FNAL/MILC 14A [75], all of which satisfy our selection criteria.

All these works have been discussed in the previous FLAG edition [76], except the new result ETM 21A, that we have already examined (and anyway does not appear in the average because it was unpublished at the deadline). The fit has $\chi^2/\mathrm{dof} \approx 2.5$, and the result shows reasonable agreement with the $N_f = 2+1$ result.

$$N_f = 2+1+1: \qquad m_s/m_{ud} = 27.23\ (10) \qquad \text{Refs. [64, 74, 75]}, \tag{38}$$

which corresponds to an overall uncertainty equal to 0.4%. It is worth noting that [74] estimates the EM effects in this quantity to be $\sim 0.18\%$ (or 0.049 which is less than the quoted error above).

All the lattice results listed in Tab. 8 as well as the FLAG averages for each value of N_f are reported in Fig. 3 and compared with χPT and sum rules.

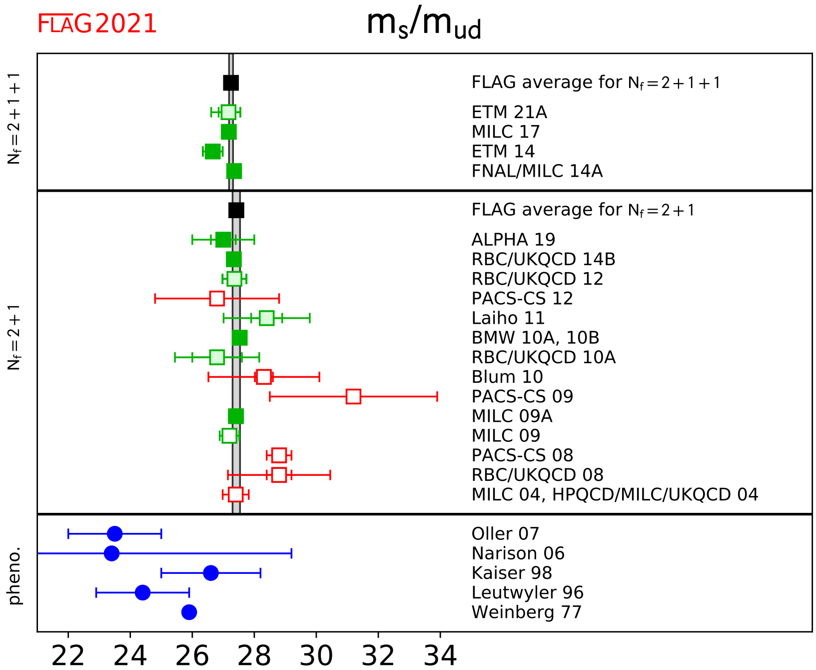

Figure 3: Results for the ratio m_s/m_{ud}. The upper part indicates the lattice results listed in Tab. 8 together with the FLAG averages for each value of N_f. The lower part shows results obtained from χPT and sum rules [71, 77–80].

3.1.6 Lattice determination of m_u and m_d

In addition to reviewing computations of individual m_u and m_d quark masses, we will also determine FLAG averages for the parameter ϵ related to the violations of Dashen's theorem

$$\epsilon = \frac{(\Delta M_K^2 - \Delta M_\pi^2)^\gamma}{\Delta M_\pi^2}\,, \tag{39}$$

where $\Delta M_\pi^2 = M_{\pi^+}^2 - M_{\pi^0}^2$ and $\Delta M_K^2 = M_{K^+}^2 - M_{K^0}^2$ are the pion and kaon squared mass splittings, respectively. The superscript γ, here and in the following, denotes corrections that arise from electromagnetic effects only. This parameter is often a crucial intermediate quantity in the extraction of the individual light-quark masses. Indeed, it can be shown, using the G-parity symmetry of the pion triplet, that ΔM_π^2 does not receive $O(\delta m)$ isospin-breaking corrections. In other words

$$\Delta M_\pi^2 = (\Delta M_\pi^2)^\gamma \qquad \text{and} \qquad \epsilon = \frac{(\Delta M_K^2)^\gamma}{\Delta M_\pi^2} - 1\,, \tag{40}$$

at leading-order in the isospin-breaking expansion. The difference $(\Delta M_\pi^2)^{SU(2)}$ was estimated in previous editions of FLAG through the ϵ_m parameter. However, consistent with our leading-order truncation of the isospin-breaking expansion, it is simpler to ignore this term. Once known, ϵ allows one to consistently subtract the electromagnetic part of the kaon-mass splitting to obtain the QCD splitting $(\Delta M_K^2)^{SU(2)}$. In contrast with the pion, the kaon QCD splitting is sensitive to δm, and, in particular, proportional to it at leading order in χPT. Therefore, the knowledge of ϵ allows for the determination of δm from a chiral fit to lattice-QCD data. Originally introduced in another form in [81], ϵ vanishes in the $SU(3)$ chiral limit, a result known as Dashen's theorem. However, in the 1990's numerous phenomenological papers pointed out that ϵ might be an $O(1)$ number, indicating a significant failure of $SU(3)$ χPT in the description of electromagnetic effects on light-meson masses. However, the phenomenological determinations of ϵ feature some level of controversy, leading to the rather imprecise estimate $\epsilon = 0.7(5)$ given in the first edition of FLAG. Starting with the FLAG 19 edition of the review, we quote more precise averages for ϵ, directly obtained from lattice-QCD+QED simulations. We refer the reader to earlier editions of FLAG and to the review [82] for discusions of the phenomenological determinations of ϵ.

The quality criteria regarding finite-volume effects for calculations including QED are presented in Sec. 2.1.1. Due to the long-distance nature of the electromagnetic interaction, these effects are dominated by a power law in the lattice spatial size. The coefficients of this expansion depend on the chosen finite-volume formulation of QED. For $\mathrm{QED_L}$, these effects on the squared mass M^2 of a charged meson are given by [18, 25, 28]

$$\Delta_{\mathrm{FV}} M^2 = \alpha M^2 \left\{ \frac{c_1}{ML} + \frac{2c_1}{(ML)^2} + \mathcal{O}\left[\frac{1}{(ML)^3}\right] \right\}\,, \tag{41}$$

with $c_1 \simeq -2.83730$. It has been shown in [18] that the two first orders in this expansion are exactly known for hadrons, and are equal to the pointlike case. However, the $\mathcal{O}[1/(ML)^3]$ term and higher orders depend on the structure of the hadron. The universal corrections for $\mathrm{QED_{TL}}$ can also be found in [18]. In all this part, for all computations using such universal formulae, the QED finite-volume quality criterion has been applied with $n_{\mathrm{min}} = 3$, otherwise $n_{\mathrm{min}} = 1$ was used.

Since FLAG 19, six new results have been reported for nondegenerate light-quark masses. In the $N_f = 2{+}1{+}1$ sector, MILC 18 [20] computed ϵ using $N_f = 2{+}1$ asqtad electro-quenched QCD+QED$_{\rm TL}$ simulations and extracted the ratio m_u/m_d from a new set of $N_f = 2+1+1$ HISQ QCD simulations. Although ϵ comes from $N_f = 2+1$ simulations, $(\Delta M_K^2)^{SU(2)}$, which is about three times larger than $(\Delta M_K^2)^{\gamma}$, has been determined in the $N_f = 2+1+1$ theory. We therefore chose to classify this result as a four-flavour one. This result is explicitly described by the authors as an update of MILC 17 [74]. In MILC 17 [74], m_u/m_d is determined as a side-product of a global analysis of heavy-meson decay constants, using a preliminary version of ϵ from MILC 18 [20]. In FNAL/MILC/TUMQCD 18 [65] the ratio m_u/m_d from MILC 17 [74] is used to determine the individual masses m_u and m_d from a new calculation of m_{ud}. The work RM123 17 [13] is the continuation of the $N_f = 2$ work named RM123 13 [12] in the previous edition of FLAG. This group now uses $N_f = 2 + 1 + 1$ ensembles from ETM 10 [83], however, still with a rather large minimum pion mass of 270 MeV, leading to the ○ rating for chiral extrapolations. In the $N_f = 2{+}1$ sector, BMW 16 [16] reuses the data set produced from their determination of the light-baryon octet-mass splittings [14] using electro-quenched QCD+QED$_{\rm TL}$ smeared clover fermion simulations. Finally, MILC 16 [84], which is a preliminary result for the value of ϵ published in MILC 18 [20], also provides a $N_f = 2 + 1$ computation of the ratio m_u/m_d.

MILC 09A [49] uses the mass difference between K^0 and K^+, from which they subtract electromagnetic effects using Dashen's theorem with corrections, as discussed in the introduction of this section. The up and down sea quarks remain degenerate in their calculation, fixed to the value of m_{ud} obtained from M_{π^0}. To determine m_u/m_d, BMW 10A, 10B [41, 42] follow a slightly different strategy. They obtain this ratio from their result for m_s/m_{ud} combined with a phenomenological determination of the isospin-breaking quark-mass ratio $Q = 22.3(8)$, from $\eta \to 3\pi$ decays [85] (the decay $\eta \to 3\pi$ is very sensitive to QCD isospin breaking, but fairly insensitive to QED isospin breaking). Instead of subtracting electromagnetic effects using phenomenology, RBC 07 [8] and Blum 10 [9] actually include a quenched electromagnetic field in their calculation. This means that their results include corrections to Dashen's theorem, albeit only in the presence of quenched electromagnetism. Since the up and down quarks in the sea are treated as degenerate, very small isospin corrections are neglected, as in MILC's calculation. PACS-CS 12 [39] takes the inclusion of isospin-breaking effects one step further. Using reweighting techniques, it also includes electromagnetic and $m_u - m_d$ effects in the sea. However, they do not correct for the large finite-volume effects coming from electromagnetism in their $M_\pi L \sim 2$ simulations, but provide rough estimates for their size, based on Ref. [24]. QCDSF/UKQCD 15 [86] uses QCD+QED dynamical simulations performed at the $SU(3)$-flavour-symmetric point, but at a single lattice spacing, so they do not enter our average. The smallest partially quenched ($m_{\rm sea} \neq m_{\rm val}$) pion mass is greater than 200 MeV, so our chiral-extrapolation criteria require a ○ rating. Concerning finite-volume effects, this work uses three spatial extents L of 1.6 fm, 2.2 fm, and 3.3 fm. QCDSF/UKQCD 15 claims that the volume dependence is not visible on the two largest volumes, leading them to assume that finite-size effects are under control. As a consequence of that, the final result for quark masses does not feature a finite-volume extrapolation or an estimation of the finite-volume uncertainty. However, in their work on the QED corrections to the hadron spectrum [86] based on the same ensembles, a volume study shows some level of compatibility with the QED$_{\rm L}$ finite-volume effects derived in [25]. We see two issues here. Firstly, the analytical result quoted from [25] predicts large, $O(10\%)$ finite-size effects from QED on the meson masses at the values of $M_\pi L$ considered in QCDSF/UKQCD 15, which is inconsistent with

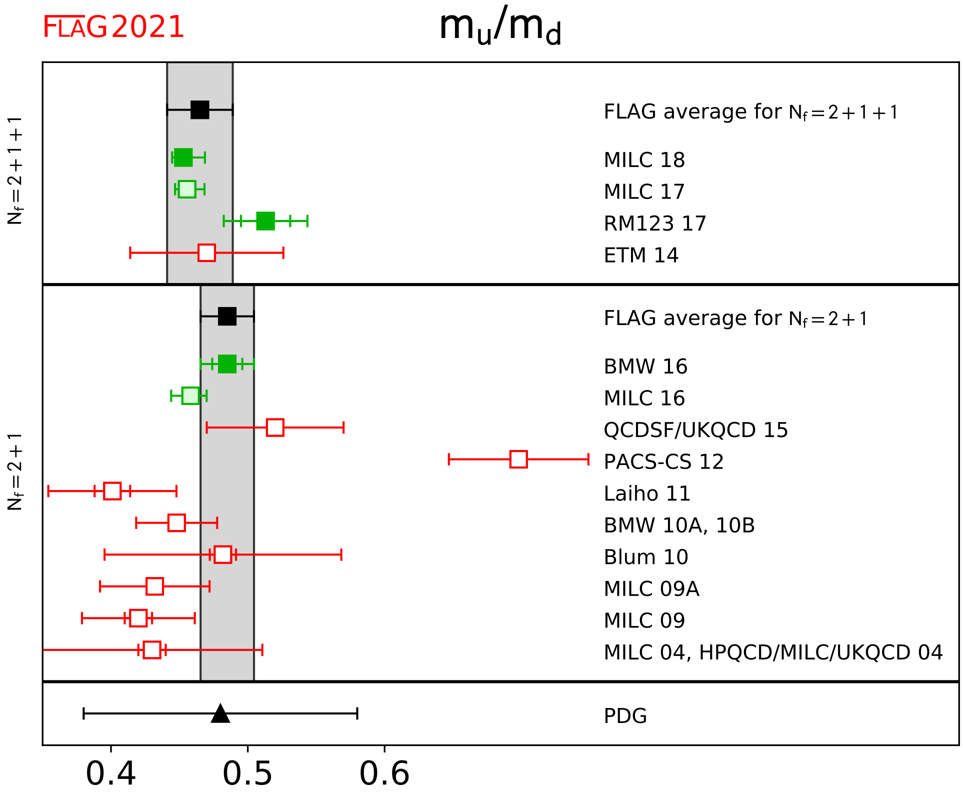

Figure 4: Lattice results and FLAG averages at $N_f = 2+1$ and $2+1+1$ for the up-down-quark masses ratio m_u/m_d, together with the current PDG estimate.

the statement made in the paper. Secondly, it is not known that the zero-mode regularization scheme used here has the same volume scaling as $\mathrm{QED_L}$. We therefore chose to assign the ■ rating for finite volume to QCDSF/UKQCD 15. Finally, for $N_f = 2+1+1$, ETM 14 [64] uses simulations in pure QCD, but determines $m_u - m_d$ from the slope $\partial M_K^2/\partial m_{ud}$ and the physical value for the QCD kaon-mass splitting taken from the phenomenological estimate in FLAG 13.

Lattice results for m_u, m_d and m_u/m_d are summarized in Tab. 9. The colour coding is specified in detail in Sec. 2.1. Considering the important progress in the last years on including isospin-breaking effects in lattice simulations, we are now in a position where averages for m_u and m_d can be made without the need of phenomenological inputs. Therefore, lattice calculations of the individual quark masses using phenomenological inputs for isospin-breaking effects will be coded ■.

We start by recalling the $N_f = 2$ FLAG average for the light-quark masses, entirely coming from RM123 13 [12],

$$N_f = 2: \qquad \begin{aligned} m_u &= 2.40(23)\,\mathrm{MeV} & \text{Ref. [12]}\,, \\ m_d &= 4.80(23)\,\mathrm{MeV} & \text{Ref. [12]}\,, \\ m_u/m_d &= 0.50(4) & \text{Ref. [12]}\,, \end{aligned} \tag{42}$$

with errors of roughly 10%, 5% and 8%, respectively. In these results, the errors are obtained by combining the lattice statistical and systematic errors in quadrature. For $N_f = 2+1$, the only result, which qualifies for entering the FLAG average for quark masses, is BMW 16 [16],

$$N_f = 2+1: \qquad \begin{aligned} m_u &= 2.27(9)\,\text{MeV} && \text{Ref. [16]}\,, \\ m_d &= 4.67(9)\,\text{MeV} && \text{Ref. [16]}\,, \\ m_u/m_d &= 0.485(19) && \text{Ref. [16]}\,, \end{aligned} \tag{43}$$

with errors of roughly 4%, 2% and 4%, respectively. This estimate is slightly more precise than in the previous edition of FLAG. More importantly, it now comes entirely from a lattice-QCD+QED calculation, whereas phenomenological input was used in previous editions. These numbers result in the following RGI averages

$$N_f = 2+1: \qquad \begin{aligned} M_u^{\rm RGI} &= 3.15(12)_m(4)_\Lambda\,\text{MeV} && \text{Ref. [16]}\,, \\ M_d^{\rm RGI} &= 6.49(12)_m(7)_\Lambda\,\text{MeV} && \text{Ref. [16]}\,. \end{aligned} \tag{44}$$

Finally, for $N_f = 2+1+1$, RM123 17 [13] and FNAL/MILC/TUMQCD 18 [65] enter the average for the individual m_u and m_d masses, and RM123 17 [13] and MILC 18 [20] enter the average for the ratio m_u/m_d, giving

$$N_f = 2+1+1: \qquad \begin{aligned} m_u &= 2.14(8)\,\text{MeV} && \text{Ref. [13, 65]}\,, \\ m_d &= 4.70(5)\,\text{MeV} && \text{Ref. [13, 65]}\,, \\ m_u/m_d &= 0.465(24) && \text{Ref. [13, 20]}\,. \end{aligned} \tag{45}$$

with errors of roughly 4%, 1% and 5%, respectively. One can observe some marginal discrepancies between results coming from the MILC collaboration and RM123 17 [13]. More specifically, adding all sources of uncertainties in quadrature, one obtains a 1.7σ discrepancy between RM123 17 [13] and MILC 18 [20] for m_u/m_d, and a 2.2σ discrepancy between RM123 17 [13] and FNAL/MILC/TUMQCD 18 [65] for m_u. However, the values of m_d and ϵ are in very good agreement between the two groups. These discrepancies are presently too weak to constitute evidence for concern, and will be monitored as more lattice groups provide results for these quantities. The RGI averages for m_u and m_d are

$$N_f = 2+1+1: \qquad \begin{aligned} M_u^{\rm RGI} &= 2.97(11)_m(3)_\Lambda\,\text{MeV} && \text{Ref. [13, 65]}\,, \\ M_d^{\rm RGI} &= 6.53(7)_m(8)_\Lambda\,\text{MeV} && \text{Ref. [13, 65]}\,. \end{aligned} \tag{46}$$

Every result for m_u and m_d used here to produce the FLAG averages relies on electro-quenched calculations, so there is some interest to comment on the size of quenching effects. Considering phenomenology and the lattice results presented here, it is reasonable for a rough estimate to use the value $(\Delta M_K^2)^\gamma \sim 2000\ \text{MeV}^2$ for the QED part of the kaon-mass splitting. Using the arguments presented in Sec. 3.1.3, one can assume that the QED sea contribution represents $O(10\%)$ of $(\Delta M_K^2)^\gamma$. Using $SU(3)$ PQχPT+QED [15, 88] gives a $\sim 5\%$ effect. Keeping the more conservative 10% estimate and using the experimental value of the kaon-mass splitting, one finds that the QCD kaon-mass splitting $(\Delta M_K^2)^{SU(2)}$ suffers from a reduced 3% quenching uncertainty. Considering that this splitting is proportional to $m_u - m_d$ at leading order in $SU(3)$ χPT, we can estimate that a similar error will propagate to the quark masses. So the individual up and down masses look mildly affected by QED quenching. However, one notices that $\sim 3\%$ is the level of error in the new FLAG averages, and increasing significantly this accuracy will require using fully unquenched calculations.

In view of the fact that a *massless up quark* would solve the strong CP problem, many authors have considered this an attractive possibility, but the results presented above exclude this possibility: the value of m_u in Eq. (43) differs from zero by 26 standard deviations. We conclude that nature solves the strong CP problem differently.

Finally, we conclude this section by giving the FLAG averages for ϵ defined in Eq. (39). For $N_f = 2+1+1$, we average the results of RM123 17 [13] and MILC 18 [20] with the value of $(\Delta M_K^2)^\gamma$ from BMW 14 [18] combined with Eq. (40), giving

$$N_f = 2+1+1: \qquad \epsilon = 0.79(6) \qquad \text{Ref. [13, 18, 20]}. \tag{47}$$

Although BMW 14 [18] focuses on hadron masses and did not extract the light-quark masses, they are the only fully unquenched QCD+QED calculation to date that qualifies to enter a FLAG average. With the exception of renormalization, which is not discussed in the paper, this work has a ★ rating for every FLAG criterion considered for the m_u and m_d quark masses. For $N_f = 2+1$ we use the results from BMW 16 [16],

$$N_f = 2+1: \qquad \epsilon = 0.73(17) \qquad \text{Ref. [16]}. \tag{48}$$

It is important to notice that the ϵ uncertainties from BMW 16 and RM123 17 are dominated by estimates of the QED quenching effects. Indeed, in contrast with the quark masses, ϵ is expected to be rather sensitive to the sea-quark QED contributions. Using the arguments presented in Sec. 3.1.3, if one conservatively assumes that the QED sea contributions represent $O(10\%)$ of $(\Delta M_K^2)^\gamma$, then Eq. (40) implies that ϵ will have a quenching error of ~ 0.15 for $(\Delta M_K^2)^\gamma \sim 2000$ MeV^2, representing a large $\sim 20\%$ relative error. It is interesting to observe that such a discrepancy does not appear between BMW 15 and RM123 17, although the $\sim 10\%$ accuracy of both results might not be sufficient to resolve these effects. On the other hand, in the context of $SU(3)$ chiral perturbation theory, Bijnens and Danielsson [15] show that the QED quenching effects on ϵ do not depend on unknown LECs at NLO and are therefore computable at that order. In that approach, MILC 18 finds the effect at NLO to be only 5%. To conclude, although the controversy around the value of ϵ has been significantly reduced by lattice-QCD+QED determinations, computing this at few-percent accuracy requires simulations with charged sea quarks.

3.1.7 Estimates for R and Q

The quark-mass ratios

$$R \equiv \frac{m_s - m_{ud}}{m_d - m_u} \quad \text{and} \quad Q^2 \equiv \frac{m_s^2 - m_{ud}^2}{m_d^2 - m_u^2} \tag{49}$$

compare $SU(3)$ breaking with isospin breaking. Both numbers only depend on the ratios m_s/m_{ud} and m_u/m_d,

$$R = \frac{1}{2}\left(\frac{m_s}{m_{ud}} - 1\right)\frac{1 + \frac{m_u}{m_d}}{1 - \frac{m_u}{m_d}} \qquad \text{and} \qquad Q^2 = \frac{1}{2}\left(\frac{m_s}{m_{ud}} + 1\right) R\,. \tag{50}$$

The quantity Q is of particular interest because of a low-energy theorem [89], which relates it to a ratio of meson masses,

$$Q_M^2 \equiv \frac{\hat{M}_K^2}{\hat{M}_\pi^2}\frac{\hat{M}_K^2-\hat{M}_\pi^2}{\hat{M}_{K^0}^2-\hat{M}_{K^+}^2}\,, \qquad \hat{M}_\pi^2 \equiv \tfrac{1}{2}(\hat{M}_{\pi^+}^2+\hat{M}_{\pi^0}^2)\,, \quad \hat{M}_K^2 \equiv \tfrac{1}{2}(\hat{M}_{K^+}^2+\hat{M}_{K^0}^2)\,. \tag{51}$$

(We remind the reader that the ˆ denotes a quantity evaluated in the $\alpha \to 0$ limit.) Chiral symmetry implies that the expansion of Q_M^2 in powers of the quark masses (i) starts with Q^2 and (ii) does not receive any contributions at NLO:

$$Q_M \overset{\text{NLO}}{=} Q\,. \tag{52}$$

We recall here the $N_f = 2$ estimates for Q and R from FLAG 16,

$$R = 40.7(3.7)(2.2)\,, \qquad\qquad Q = 24.3(1.4)(0.6)\ , \tag{53}$$

where the second error comes from the phenomenological inputs that were used. For $N_f = 2+1$, we use Eqs. (37) and (43) and obtain

$$R = 38.1(1.5)\,, \qquad\qquad Q = 23.3(0.5)\ , \tag{54}$$

where now only lattice results have been used. For $N_f = 2+1+1$ we obtain

$$R = 35.9(1.7)\,, \qquad\qquad Q = 22.5(0.5)\ , \tag{55}$$

which are quite compatible with two- and three-flavour results. It is interesting to notice that the most recent phenomenological determination of R and Q from $\eta \to 3\pi$ decay [90] gives the values $R = 34.4(2.1)$ and $Q = 22.1(7)$, which are marginally discrepant with some of the averages presented here. The authors of [90, 91] point out that this discrepancy is likely due to surprisingly large corrections to the approximation in Eq. (52) used in the phenomenological analysis.

Our final results for the masses m_u, m_d, m_{ud}, m_s and the mass ratios m_u/m_d, m_s/m_{ud}, R, Q are collected in Tabs. 10 and 11.

Collaboration	Ref.	publication status	chiral extrapolation	continuum extrapolation	finite volume	renormalization	running	m_{ud}	m_s
ALPHA 19	[36]	A	○	★	★	★	e	3.54(12)(9)	95.7(2.5)(2.4)
Maezawa 16	[37]	A	■	★	★	★	d	–	92.0(1.7)
RBC/UKQCD 14B$^{\ominus}$	[38]	A	★	★	★	★	d	3.31(4)(4)	90.3(0.9)(1.0)
RBC/UKQCD 12$^{\ominus}$	[35]	A	★	○	★	★	d	3.37(9)(7)(1)(2)	92.3(1.9)(0.9)(0.4)(0.8)
PACS-CS 12*	[39]	A	★	■	■	★	b	3.12(24)(8)	83.60(0.58)(2.23)
Laiho 11	[40]	C	○	★	★	○	–	3.31(7)(20)(17)	94.2(1.4)(3.2)(4.7)
BMW 10A, 10B^{+}	[41, 42]	A	★	★	★	★	c	3.469(47)(48)	95.5(1.1)(1.5)
PACS-CS 10	[43]	A	★	■	■	★	b	2.78(27)	86.7(2.3)
MILC 10A	[44]	C	○	★	★	○	–	3.19(4)(5)(16)	–
HPQCD 10**	[45]	A	○	★	★	–	–	3.39(6)	92.2(1.3)
RBC/UKQCD 10A	[46]	A	○	○	★	★	a	3.59(13)(14)(8)	96.2(1.6)(0.2)(2.1)
Blum 10†	[9]	A	○	■	○	★	–	3.44(12)(22)	97.6(2.9)(5.5)
PACS-CS 09	[47]	A	★	■	■	★	b	2.97(28)(3)	92.75(58)(95)
HPQCD 09A$^{\oplus}$	[48]	A	○	★	★	–	–	3.40(7)	92.4(1.5)
MILC 09A	[49]	C	○	★	★	○	–	3.25 (1)(7)(16)(0)	89.0(0.2)(1.6)(4.5)(0.1)
MILC 09	[50]	A	○	★	★	○	–	3.2(0)(1)(2)(0)	88(0)(3)(4)(0)
PACS-CS 08	[51]	A	★	■	■	■	–	2.527(47)	72.72(78)
RBC/UKQCD 08	[52]	A	○	■	★	★	–	3.72(16)(33)(18)	107.3(4.4)(9.7)(4.9)
CP-PACS/ JLQCD 07	[53]	A	■	★	★	■	–	$3.55(19)(^{+56}_{-20})$	$90.1(4.3)(^{+16.7}_{-4.3})$
HPQCD 05	[54]	A	○	○	○	○	–	$3.2(0)(2)(2)(0)^{\ddagger}$	$87(0)(4)(4)(0)^{\ddagger}$
MILC 04, HPQCD/ MILC/UKQCD 04	[55, 56]	A	○	○	○	■	–	2.8(0)(1)(3)(0)	76(0)(3)(7)(0)

$^{\ominus}$ The results are given in the $\overline{\rm MS}$ scheme at 3 instead of 2 GeV. We run them down to 2 GeV using numerically integrated 4-loop running [57, 58] with $N_f = 3$ and with the values of $\alpha_s(M_Z)$, m_b, and m_c taken from Ref. [59]. The running factor is 1.106. At three loops it is only 0.2% smaller, indicating that perturbative running uncertainties are small. We neglect them here.

* The calculation includes electromagnetic and $m_u \neq m_d$ effects through reweighting.

$^{+}$ The fermion action used is tree-level improved.

** m_s is obtained by combining m_c and HPQCD 09A's $m_c/m_s = 11.85(16)$ [48]. Finally, m_{ud} is determined from m_s with the MILC 09 result for m_s/m_{ud}. Since m_c/m_s is renormalization group invariant in QCD, the renormalization and running of the quark masses enter indirectly through that of m_c (see below).

† The calculation includes quenched electromagnetic effects.

$^{\oplus}$ What is calculated is $m_c/m_s = 11.85(16)$. m_s is then obtained by combining this result with the determination $m_c(m_c) = 1.268(9)$ GeV from Ref. [60]. Finally, m_{ud} is determined from m_s with the MILC 09 result for m_s/m_{ud}.

‡ The bare numbers are those of MILC 04. The masses are simply rescaled, using the ratio of the 2-loop to 1-loop renormalization factors.

a The masses are renormalized nonperturbatively at a scale of 2 GeV in a couple of $N_f = 3$ RI-SMOM schemes. A careful study of perturbative matching uncertainties has been performed by comparing results in the two schemes in the region of 2 GeV to 3 GeV [46].

b The masses are renormalized and run nonperturbatively up to a scale of 40 GeV in the $N_f = 3$ SF scheme. In this scheme, nonperturbative and NLO running for the quark masses are shown to agree well from 40 GeV all the way down to 3 GeV [43].

c The masses are renormalized and run nonperturbatively up to a scale of 4 GeV in the $N_f = 3$ RI-MOM scheme. In this scheme, nonperturbative and N^{3}LO running for the quark masses are shown to agree from 6 GeV down to 3 GeV to better than 1% [42].

d All required running is performed nonperturbatively.

e Running is performed nonperturbatively from 200 MeV to the electroweak scale ~ 100 GeV.

Table 6: $N_f = 2+1$ lattice results for the masses m_{ud} and m_s (MeV).

Collaboration	Ref.	publication status	chiral extrapolation	continuum extrapolation	finite volume	renormalization	running	m_{ud}	m_s
ETM 21A	[63]	P	★	★	★	★	–	$3.636(66)(^{+60}_{-57})$	$98.7(2.4)(^{+4.0}_{-3.2})$
HPQCD 18†	[66]	A	★	★	★	★	–		94.49(96)
FNAL/MILC/TUMQCD 18	[65]	A	★	★	★	★	–	3.404(14)(21)	92.52(40)(56)
HPQCD 14A ⊕	[67]	A	★	★	★	–	–		93.7(8)
ETM 14⊕	[64]	A	○	★	★	★	–	3.70(13)(11)	99.6(3.6)(2.3)

† Bare-quark masses are renormalized nonperturbatively in the RI-SMOM scheme at scales $\mu \sim 2-5$ GeV for different lattice spacings and translated to the $\overline{\rm MS}$ scheme. Perturbative running is then used to run all results to a reference scale $\mu = 3$ GeV.

⊕ As explained in the text, m_s is obtained by combining the results $m_c(5\,\mathrm{GeV}; N_f = 4) = 0.8905(56)$ GeV and $(m_c/m_s)(N_f = 4) = 11.652(65)$, determined on the same data set. A subsequent scale and scheme conversion, performed by the authors, leads to the value 93.6(8). In the table, we have converted this to $m_s(2\,\mathrm{GeV}; N_f = 4)$, which makes a very small change.

Table 7: $N_f = 2 + 1 + 1$ lattice results for the masses m_{ud} and m_s (MeV).

Collaboration	Ref.	N_f	publication status	chiral extrapolation	continuum extrapolation	finite volume	m_s/m_{ud}
ETM 21A	[63]	2+1+1	P	★	★	★	$27.17(32)^{+56}_{-38}$
MILC 17 ‡	[74]	2+1+1	A	★	★	★	$27.178(47)^{+86}_{-57}$
FNAL/MILC 14A	[75]	2+1+1	A	★	★	★	$27.35(5)^{+10}_{-7}$
ETM 14	[64]	2+1+1	A	○	★	○	26.66(32)(2)
RBC/UKQCD 14B	[38]	2+1	A	★	★	★	27.34(21)
RBC/UKQCD 12⊖	[35]	2+1	A	★	○	★	27.36(39)(31)(22)
PACS-CS 12⋆	[39]	2+1	A	★	■	■	26.8(2.0)
Laiho 11	[40]	2+1	C	○	★	★	28.4(0.5)(1.3)
BMW 10A, 10B+	[41, 42]	2+1	A	★	★	★	27.53(20)(8)
RBC/UKQCD 10A	[46]	2+1	A	○	○	★	26.8(0.8)(1.1)
Blum 10†	[9]	2+1	A	○	■	○	28.31(0.29)(1.77)
PACS-CS 09	[47]	2+1	A	★	■	■	31.2(2.7)
MILC 09A	[49]	2+1	C	○	★	★	27.41(5)(22)(0)(4)
MILC 09	[50]	2+1	A	○	★	★	27.2(1)(3)(0)(0)
PACS-CS 08	[51]	2+1	A	★	■	■	28.8(4)
RBC/UKQCD 08	[52]	2+1	A	○	■	★	28.8(0.4)(1.6)
MILC 04, HPQCD/ MILC/UKQCD 04	[55, 56]	2+1	A	○	○	○	27.4(1)(4)(0)(1)

‡ The calculation includes electromagnetic effects.
⊖ The errors are statistical, chiral and finite volume.
⋆ The calculation includes electromagnetic and $m_u \neq m_d$ effects through reweighting.
+ The fermion action used is tree-level improved.
† The calculation includes quenched electromagnetic effects.

Table 8: Lattice results for the ratio m_s/m_{ud}.

Collaboration	Ref.	publication status	chiral extrapolation	continuum extrapolation	finite volume	isospin breaking	renormalization	running	m_u	m_d	m_u/m_d
MILC 18	[20]	A	★	★	★	○	★	–			$0.4529(48)(^{+150}_{-67})$
FNAL/MILC/TUMQCD 18*	[65]	A	★	★	★	○	★	–	2.118(17)(32)(12)(03)	4.690(30)(36)(26)(06)	
MILC 17†	[74]	A	★	★	★	○	★	–			$0.4556(55)(^{+114}_{-67})(13)$
RM123 17	[13]	A	○	★	★	○	★	b	2.50(15)(8)(2)	4.88(18)(8)(2)	0.513(18)(24)(6)
ETM 14	[64]	A	★	★	★	■	★	b	2.36(24)	5.03(26)	0.470(56)
BMW 16	[16]	A	★	★	★	○	★	–	2.27(6)(5)(4)	4.67(6)(5)(4)	0.485(11)(8)(14)
MILC 16	[84]	C	○	★	★	○	★	–			$0.4582(38)(^{+12}_{-82})(1)(110)$
QCDSF/UKQCD 15	[86]	A	○	■	■	★	–	–			0.52(5)
PACS-CS 12	[39]	A	★	■	■	★	★	a	2.57(26)(7)	3.68(29)(10)	0.698(51)
Laiho 11	[40]	C	○	★	★	■	○	–	1.90(8)(21)(10)	4.73(9)(27)(24)	0.401(13)(45)
HPQCD 10‡	[45]	A	○	★	★	■	★	–	2.01(14)	4.77(15)	
BMW 10A, 10B+	[41, 42]	A	★	★	★	■	★	b	2.15(03)(10)	4.79(07)(12)	0.448(06)(29)
Blum 10	[9]	A	○	■	○	○	★	–	2.24(10)(34)	4.65(15)(32)	0.4818(96)(860)
MILC 09A	[49]	C	○	★	★	■	○	–	1.96(0)(6)(10)(12)	4.53(1)(8)(23)(12)	0.432(1)(9)(0)(39)
MILC 09	[50]	A	○	★	★	■	○	–	1.9(0)(1)(1)(1)	4.6(0)(2)(2)(1)	0.42(0)(1)(0)(4)
MILC 04, HPQCD/ MILC/UKQCD 04	[55][56]	A	○	○	○	■	■	–	1.7(0)(1)(2)(2)	3.9(0)(1)(4)(2)	0.43(0)(1)(0)(8)

* FNAL/MILC/TUMQCD 18 uses ϵ from MILC 18 to produce the individual m_u and m_d masses.

† MILC 17 additionally quotes an optional 0.0032 uncertainty on m_u/m_d corresponding to QED and QCD separation scheme ambiguities. Because this variation is not per se an error on the determination of m_u/m_d, and because it is generally not included in other results, we choose to omit it here.

‡ Values obtained by combining the HPQCD 10 result for m_s with the MILC 09 results for m_s/m_{ud} and m_u/m_d.

+ The fermion action used is tree-level improved.

a The masses are renormalized and run nonperturbatively up to a scale of 100 GeV in the $N_f = 2$ SF scheme. In this scheme, nonperturbative and NLO running for the quark masses are shown to agree well from 100 GeV all the way down to 2 GeV [87].

b The masses are renormalized and run nonperturbatively up to a scale of 4 GeV in the $N_f = 3$ RI-MOM scheme. In this scheme, nonperturbative and N^{3}LO running for the quark masses are shown to agree from 6 GeV down to 3 GeV to better than 1% [42].

Table 9: Lattice results for m_u, m_d (MeV) and for the ratio m_u/m_d. The values refer to the $\overline{\mathrm{MS}}$ scheme at scale 2 GeV. The top part of the table lists the results obtained with $N_f = 2+1+1$, while the lower part presents calculations with $N_f = 2+1$.

N_f	m_{ud}	m_s	m_s/m_{ud}
2+1+1	3.410(43)	93.44(68)	27.23(10)
2+1	3.364(41)	92.03(88)	27.42(12)

Table 10: Our estimates for the strange-quark and the average up-down-quark masses in the $\overline{\mathrm{MS}}$ scheme at running scale $\mu = 2\,\mathrm{GeV}$. Mass values are given in MeV. In the results presented here, the error is the one which we obtain by applying the averaging procedure of Sec. 2.3 to the relevant lattice results.

N_f	m_u	m_d	m_u/m_d	R	Q
2+1+1	2.14(8)	4.70(5)	0.465(24)	35.9(1.7)	22.5(0.5)
2+1	2.27(9)	4.67(9)	0.485(19)	38.1(1.5)	23.3(0.5)

Table 11: Our estimates for the masses of the two lightest quarks and related, strong isospin-breaking ratios. Again, the masses refer to the $\overline{\mathrm{MS}}$ scheme at running scale $\mu = 2\,\mathrm{GeV}$. Mass values are given in MeV.

3.2 Charm-quark mass

In the following, we collect and discuss the lattice determinations of the $\overline{\mathrm{MS}}$ charm-quark mass $\overline{m}_c$. Most of the results have been obtained by analyzing the lattice-QCD simulations of two-point heavy-light- or heavy-heavy-meson correlation functions, using as input the experimental values of the D, D_s, and charmonium mesons. Some groups use the moments method. The latter is based on the lattice calculation of the Euclidean time moments of pseudoscalar-pseudoscalar correlators for heavy-quark currents followed by an OPE expansion dominated by perturbative QCD effects, which provides the determination of both the heavy-quark mass and the strong-coupling constant α_s.

The heavy-quark actions adopted by various lattice collaborations have been discussed in previous FLAG reviews [6, 76, 92], and their descriptions can be found in Sec. A.1.3 of FLAG 19 [76]. While the charm mass determined with the moments method does not need any lattice evaluation of the mass-renormalization constant Z_m, the extraction of $\overline{m}_c$ from two-point heavy-meson correlators does require the nonperturbative calculation of Z_m. The lattice scale at which Z_m is obtained is usually at least of the order 2–3 GeV, and therefore it is natural in this review to provide the values of $\overline{m}_c(\mu)$ at the renormalization scale $\mu = 3$ GeV. Since the choice of a renormalization scale equal to $\overline{m}_c$ is still commonly adopted (as by the PDG [1]), we have collected in Tab. 12 the lattice results for both $\overline{m}_c(\overline{m}_c)$ and $\overline{m}_c(3\text{ GeV})$, obtained for $N_f = 2+1$ and $2+1+1$. For $N_f = 2$, interested readers are referred to previous reviews [6, 92].

When not directly available in the published work, we apply a conversion factor using perturbative QCD evolution at five loops to run down from $\mu = 3$ GeV to the scales $\mu = \overline{m}_c$ and 2 GeV of 0.7393(60) and 0.9026(23), respectively, where the error comes from the uncertainty in $\Lambda_{\rm QCD}$. We use $\Lambda_{\rm QCD} = 297(12)$ MeV for $N_f = 4$ (see Sec. 9). Perturbation theory uncertainties, estimated as the difference between results that use 4- and 5-loop running, are significantly smaller than the parametric uncertainty coming from $\Lambda_{\rm QCD}$. For $\mu = \overline{m}_c$, the former is about about 2.5 times smaller. Given the high precision of many of these results, future works should take the uncertainties in $\Lambda_{\rm QCD}$ and perturbation theory seriously.

In the next subsections we review separately the results for $\overline{m}_c$ with three or four flavours of quarks in the sea.

3.2.1 $N_f = 2+1$ results

Since the last review [76], there are two new results, Petreczky 19 [96] and ALPHA 21 [95], the latter of which was not published at the FLAG deadline. Petreczky 19 employs the HISQ action on ten ensembles with ten lattice spacings down to 0.025 fm, physical strange-quark mass, and two light-quark masses, the lightest corresponding to 161 MeV pions. Their study incorporates lattices with 11 different sizes, ranging from 1.6 to 5.4 fm. The masses are computed from moments of pseudoscalar quarkonium correlation functions, and $\overline{\mathrm{MS}}$ masses are extracted with 4-loop continuum perturbation theory. Thus this work easily rates green stars in all categories. ALPHA 21 uses the $\mathcal{O}(a)$-improved Wilson-clover action with five lattice spacings from 0.087 to 0.039 fm, produced by the CLS collaboration. For each lattice spacing, several light sea-quark masses are used in a global chiral-continuum extrapolation (the lightest pion mass for one ensemble is 198 MeV). The authors also use nonperturbative renormalization and running through application of step-scaling and the Schrödinger functional scheme. Finite-volume effects are investigated at one lattice spacing and only for ~ 400

Collaboration	Ref.	N_f	publication status	chiral extrapolation	continuum extrapolation	finite volume	renormalization	$\overline{m}_c(\overline{m}_c)$	$\overline{m}_c(3\text{ GeV})$
ETM 21A	[63]	2+1+1	P	★	★	★	★	$1.401(22)(^{+19}_{-10})(11)^\dagger$	$1.036(17)(^{+15}_{-8})$
HPQCD 20A	[93]	2+1+1	A	★	★	★	★	1.2719(78)	0.9841(51)
HPQCD 18	[66]	2+1+1	A	★	★	★	★	1.2757(84)	0.9896(61)
FNAL/MILC/ TUMQCD 18	[65]	2+1+1	A	★	★	★	–	1.273(4)(1)(10)	0.9837(43)(14)(33)(5)
HPQCD 14A	[67]	2+1+1	A	★	★	★	–	1.2715(95)	0.9851(63)
ETM 14A	[94]	2+1+1	A	○	★	○	★	1.3478(27)(195)	1.0557(22)(153)
ETM 14	[64]	2+1+1	A	○	★	○	★	1.348(46)	1.058(35)
ALPHA 21	[95]	2+1	A^+	★	★	★	★	1.296(19)	1.007(16)
Petreczky 19	[96]	2+1	A	★	★	★	★	1.265(10)	1.001(16)
Maezawa 16	[37]	2+1	A	■	★	★	★	1.267(12)	
JLQCD 16	[97]	2+1	A	○	★	★	–	1.2871(123)	1.0033(96)
χQCD 14	[98]	2+1	A	○	○	○	★	1.304(5)(20)	1.006(5)(22)
HPQCD 10	[45]	2+1	A	○	★	○	–	1.273(6)	0.986(6)
HPQCD 08B	[60]	2+1	A	○	★	○	–	1.268(9)	0.986(10)
PDG	[1]							1.27(2)	

† We applied the running factor 0.7393(60) for $\mu = 3$ GeV to $\overline{m}_c$. The errors are statistical, systematic, and the uncertainty in the running factor.
+ Published after the FLAG deadline.

Table 12: Lattice results for the $\overline{\text{MS}}$ charm-quark mass $\overline{m}_c(\overline{m}_c)$ and $\overline{m}_c(3\text{ GeV})$ in GeV, together with the colour coding of the calculations used to obtain them.

MeV pions on the smallest two volumes where results are compatible within statistical errors. ALPHA 21 satisfies the FLAG criteria for green-star ratings in all of the categories listed in Tab. 12, but because it is a new result that was unpublished at the deadline, does not enter the average in this review.

Descriptions of the other works in this section can be found in the last review [76].

According to our rules on the publication status, the FLAG average for the charm-quark mass at $N_f = 2+1$ is obtained by combining the results HPQCD 10, χQCD 14, JLQCD 16, and Petreczky 19,

$$N_f = 2+1: \qquad \overline{m}_c(\overline{m}_c) = 1.275(5)\text{ GeV} \qquad \text{Refs. [45, 96–98]}, \tag{56}$$
$$\overline{m}_c(3\text{ GeV}) = 0.992(5)\text{ GeV} \qquad \text{Refs. [45, 96–98]}, \tag{57}$$

where the error on $\overline{m}_c(\overline{m}_c)$ includes a stretching factor $\sqrt{\chi^2/\text{dof}} \simeq 1.16$ as discussed in Sec. 2.2. This result corresponds to the following RGI average

$$M_c^{\text{RGI}} = 1.526(9)_m(14)_\Lambda\text{ GeV} \qquad \text{Refs. [45, 96–98]}. \tag{58}$$

3.2.2 $N_f = 2+1+1$ results

For a discussion of older results, see the previous FLAG reviews. Since FLAG 19 two groups have produced updated values with charm quarks in the sea.

HPQCD 20A [93] is an update of HPQCD 18, including a new finer ensemble ($a \approx 0.045$ fm) and EM corrections computed in the quenched approximation of QED for the first time. Besides these new items, the analysis is largely unchanged from HPQCD 18 except for an added α_s^3 correction to the SMOM-to-$\overline{\rm MS}$ conversion factor and tuning the bare charm mass via the J/ψ mass rather than the η_c. Their new value in pure QCD is $\overline{m}_c(3~\text{GeV}) = 0.9858(51)$ GeV which is quite consistent with HPQCD 18 and the FLAG 19 average. The effects of quenched QED in both the bare charm-quark mass and the renormalization constant are small. Both effects are precisely determined, and the overall effect shifts the mass down slightly to $\overline{m}_c(3~\text{GeV}) = 0.9841(51)$ where the uncertainty due to QED is invisible in the final error. The shift from their pure QCD value due to quenched QED is about -0.2%.

ETM 21A [63] is a new work that follows a similar methodology as ETM 14, but with significant improvements. Notably, a clover-term is added to the twisted mass fermion action which suppresses $\mathcal{O}(a^2)$ effects between the neutral and charged pions. Additional improvements include new ensembles lying very close to the physical mass point, better control of nonperturbative renormalization systematics, and use of both meson and baryon correlation functions to determine the quark mass. They use the RI-MOM scheme for nonperturbative renormalization. The analysis comprises ten ensembles in total with three lattice spacings (0.095, 0.082, and 0.069 fm), two volumes for the finest lattice spacings and four for the other two, and pion masses down to 134 MeV for the finest ensemble. The values of $m_\pi L$ range mostly from almost four to greater than five. According to the FLAG criteria, green stars are earned in all categories. The authors find $m_c(3~\text{GeV}) = 1.036(17)(^{+15}_{-8})$ GeV. In Tab. 12 we have applied a factor of 0.770 to run from 3 GeV to $\overline{m}_c$. As in FLAG 19, the new value is consistent with ETM 14 and ETM 14A, but is still high compared to the FLAG average. The authors plan future improvements, including a finer lattice spacing for better control of the continuum limit and a new renormalization scheme, like RI-SMOM. This result has not been published by the deadline, so it does not yet appear in the average.

Five results enter the FLAG average for $N_f = 2+1+1$ quark flavours: ETM 14, ETM 14A, HPQCD 14A, FNAL/MILC/TUMQCD 18, and HPQCD 20A. We note that while the determinations of $\overline{m}_c$ by ETM 14 and 14A agree well with each other, they are incompatible with HPQCD 14A, FNAL/MILC/TUMQCD 18, and HPQCD 20A by several standard deviations. While the latter use the same configurations, the analyses are quite different and independent. As mentioned earlier, m_{ud} and m_s values by ETM are also systematically high compared to their respective averages. Combining all four results yields

$$N_f = 2+1+1: \qquad \overline{m}_c(\overline{m}_c) = 1.278(13)\text{GeV} \qquad \text{Refs. [64, 65, 67, 93, 94]}, \tag{59}$$

$$\overline{m}_c(3~\text{GeV}) = 0.988(11)~\text{GeV} \qquad \text{Refs. [64, 65, 67, 93, 94]}, \tag{60}$$

where the errors include large stretching factors $\sqrt{\chi^2/\text{dof}} \approx 2.0$ and 2.5, respectively. We have assumed 100% correlation for statistical errors between ETM results and the same for HPQCD 14A, HPQCD 20A, and FNAL/MILC/TUMQCD 18.

These are obviously poor χ^2 values, and the stretching factors are quite large. While it may be prudent in such a case to quote a range of values covering the central values of all results that pass the quality criteria, we believe in this case that would obscure rather than clarify the situation. From Fig. 5 we note that not only do ETM 21A, ETM 14A, and ETM 14 lie well above the other 2+1+1 results, but also above all of the 2+1 flavour results. A similar trend is apparent for the light-quark masses (see Figs. 1 and 2) while for mass ratios there is better agreement (Figs. 3, 4 and 6). The latter suggests there may be underestimated systematic uncertainties associated with scale setting and/or renormalization which have not been detected. Finally we note the ETM results are significantly higher than the PDG average. For these reasons, which admittedly are not entirely satisfactory, we continue to quote an average with a stretching factor as in previous reviews.

The RGI average reads as follows,

$$M_c^{\rm RGI} = 1.520(17)_m(14)_\Lambda \text{ GeV} \qquad \text{Refs. [64, 65, 67, 93, 94]}. \tag{61}$$

Figure 5 presents the values of $\overline{m}_c(\overline{m}_c)$ given in Tab. 12 along with the FLAG averages obtained for $2+1$ and $2+1+1$ flavours.

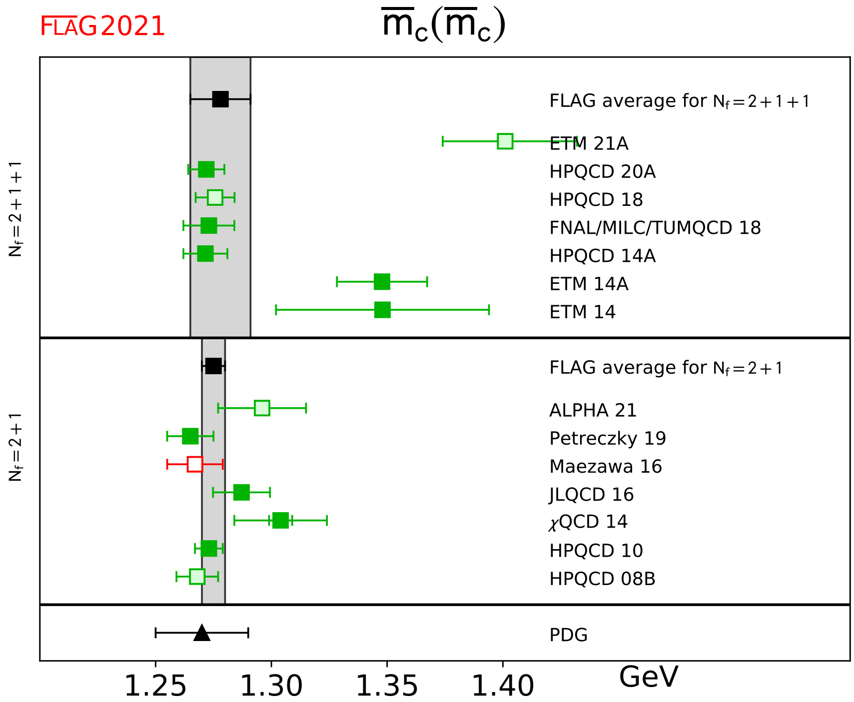

Figure 5: The charm-quark mass for $2+1$ and $2+1+1$ flavours. For the latter a large stretching factor is used for the FLAG average due to poor χ^2 from our fit.

3.2.3 Lattice determinations of the ratio m_c/m_s

Because some of the results for quark masses given in this review are obtained via the quark-mass ratio m_c/m_s, we review these lattice calculations, which are listed in Tab. 13, as well.

The $N_f = 2+1$ results from χQCD 14 and HPQCD 09A [48] are from the same calculations that were described for the charm-quark mass in the previous review. Maezawa 16 does not pass our chiral-limit test (see the previous review), though we note that it is quite consistent with the other values. Combining χQCD 14 and HPQCD 09A, we obtain the same result reported in FLAG 19,

$$N_f = 2+1: \qquad m_c/m_s = 11.82(16) \qquad \text{Refs. [48, 98]}, \tag{62}$$

Collaboration	Ref.	N_f	publication status	chiral extrapolation	continuum extrapolation	finite volume	m_c/m_s
ETM 21A	[63]	2+1+1	P	★	★	★	$11.48(12)(^{+25}_{-19})$
FNAL/MILC/TUMQCD 18	[65]	2+1+1	A	★	★	★	11.784(11)(17)(00)(08)
HPQCD 14A	[67]	2+1+1	A	★	★	★	11.652(35)(55)
FNAL/MILC 14A	[75]	2+1+1	A	★	★	★	$11.747(19)(^{+59}_{-43})$
ETM 14	[64]	2+1+1	A	○	★	○	11.62(16)
Maezawa 16	[37]	2+1	A	■	★	★	11.877(91)
χQCD 14	[98]	2+1	A	○	○	○	11.1(8)
HPQCD 09A	[48]	2+1	A	○	★	★	11.85(16)

Table 13: Lattice results for the quark-mass ratio m_c/m_s, together with the colour coding of the calculations used to obtain them.

with a $\chi^2/\mathrm{dof} \simeq 0.85$.

Turning to $N_f = 2+1+1$, there is a new result from ETM 21A. The errors have actually increased compared to ETM 14, due to larger uncertainties in the baryon sector which enter their average with the meson sector. Again, ETM 21A does not yet enter the average since it was not published by the deadline for the review. See the earlier reviews for a discussion of previous results.

We note that some tension exists between the HPQCD 14A and FNAL/MILC/TUMQCD results. Combining these with ETM 14 yields

$$N_f = 2+1+1: \qquad m_c/m_s = 11.768(34) \qquad \text{Refs. [64, 65, 67]}, \tag{63}$$

where the error includes the stretching factor $\sqrt{\chi^2/\mathrm{dof}} \simeq 1.5$. We have assumed a 100% correlation of statistical errors for FNAL/MILC/TUMQCD 18 and HPQCD 14A.

Results for m_c/m_s are shown in Fig. 6 together with the FLAG averages for $N_f = 2+1$ and $2+1+1$ flavours.

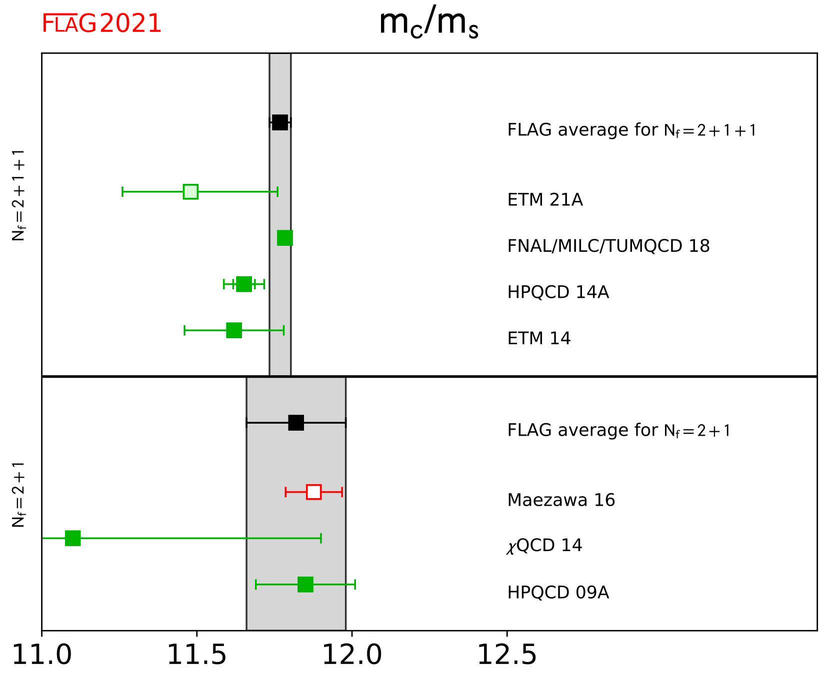

Figure 6: Lattice results for the ratio m_c/m_s listed in Tab. 13 and the FLAG averages corresponding to $2+1$ and $2+1+1$ quark flavours. The latter average includes a large stretching factor on the error due a poor χ^2 from our fit.

3.3 Bottom-quark mass

Now we review the lattice results for the $\overline{\text{MS}}$ bottom-quark mass $\overline{m}_b$. Related heavy-quark actions and observables have been discussed in previous FLAG reviews [6, 76, 92], and descriptions can be found in Sec. A.1.3 of FLAG 19 [76]. In Tab. 14 we collect results for $\overline{m}_b(\overline{m}_b)$ obtained with $N_f = 2+1$ and $2+1+1$ sea-quark flavours. Available results for the quark-mass ratio m_b/m_c are also reported. After discussing the new results we evaluate the corresponding FLAG averages.

3.3.1 $N_f = 2+1$

There is one new three-flavour result since the last review, Petreczky 19, which was described already in the charm-quark section. The new result rates green stars, so our new average with HPQCD 10 is (both works quote values in the $N_f = 5$ theory, so we simply use those values),

$$N_f = 2+1: \qquad \overline{m}_b(\overline{m}_b) = 4.171(20)\ \text{GeV} \qquad \text{Ref. [45, 96]}. \tag{64}$$

The corresponding four-flavour RGI average is

$$N_f = 2+1: \qquad M_b^{\text{RGI}} = 6.881(33)_m(54)_\Lambda\ \text{GeV} \qquad \text{Ref. [45, 96]}. \tag{65}$$

Collaboration	Ref.	N_f	publication status	chiral extrapolation	continuum extrapolation	finite volume	renormalization	heavy-quark treatment	$\overline{m}_b(\overline{m}_b)$	m_b/m_c
HPQCD 21	[99]	2+1+1	A	★	★	★	–	✓	$4.209(21)^{++}$	$4.586(12)^{**}$
FNAL/MILC/TUM 18	[65]	2+1+1	A	★	○	★	–	✓	4.201(12)(1)(8)(1)	4.578(5)(6)(0)(1)
Gambino 17	[100]	2+1+1	A	○	★	○	★	✓	4.26(18)	
ETM 16B	[101]	2+1+1	A	○	★	○	★	✓	$4.26(3)(10)^{+}$	4.42(3)(8)
HPQCD 14B	[102]	2+1+1	A	★	★	★	★	✓	$4.196(0)(23)^{\dagger}$	
ETM 14B	[103]	2+1+1	C	○	★	○	★	✓	4.26(7)(14)	4.40(6)(5)
HPQCD 14A	[67]	2+1+1	A	★	★	★	–	✓	4.162(48)	4.528(14)(52)
Petreczky19	[96]	2+1	A	★	★	★	★	✓	4.188(37)	4.586(43)
Maezawa 16	[37]	2+1	A	■	★	★	★	✓	4.184(89)	4.528(57)
HPQCD 13B	[104]	2+1	A	■	○	–	–	✓	4.166(43)	
HPQCD 10	[45]	2+1	A	★	★	★	–	✓	$4.164(23)^{\star}$	4.51(4)
ETM 13B	[105]	2	A	○	★	○	★	✓	4.31(9)(8)	
ALPHA 13C	[106]	2	A	★	★	★	★	✓	4.21(11)	
ETM 11A	[107]	2	A	○	★	○	★	✓	4.29(14)	
PDG	[1]								$4.18^{+0.02}_{-0.03}$	

$^{++}$ We quote the four-flavour result. For $N_f = 5$, value is 4.202(21).
** The ratio is quoted in the $\overline{\rm MS}$ scheme for $\mu = 3$ GeV because of the different charges of the bottom and charm quarks.
$^{+}$ The lattice spacing used in ETM 14B has been updated here.
† Only two pion points are used for chiral extrapolation.
* The number that is given is $m_b(10\text{ GeV}, N_f = 5) = 3.617(25)$ GeV.

Table 14: Lattice results for the $\overline{\rm MS}$ bottom-quark mass $\overline{m}_b(\overline{m}_b)$ in GeV, together with the systematic error ratings for each. Available results for the quark-mass ratio m_b/m_c are also reported.

3.3.2 $N_f = 2+1+1$

HPQCD 21 [99] is an update of HPQCD 14A (and replaces it in our average), including EM corrections for the first time for the b-quark mass. Four flavours of HISQ quarks are used on MILC ensembles with lattice spacings from about 0.09 to 0.03 fm. Ensembles with physical and unphysical mass sea-quarks are used. Quenched QED is used to obtain the dominant O(α) effect. The ratio of bottom- to charm-quark masses is computed in a completely non-perturbative formulation, and the b-quark mass is extracted using the value of $\overline{m}_c$(3 GeV) from HPQCD 20A. Since EM effects are included, the QED renormalization scale enters the ratio which is quoted for 3 GeV and $N_f = 4$. The total error on the new result is more than two times smaller than for HPQCD 14A, but is only slightly smaller compared to the NRQCD result reported in HPQCD 14B. The inclusion of QED shifts the ratio m_b/m_c up slightly from the pure QCD value by about one standard deviation, and the value of $\overline{m}_b(m_b)$ is consistent, within errors, to the other pure QCD results entering our average. Therefore we quote a single average.

HPQCD 14B employs the NRQCD action [102] to treat the b quark. The b-quark mass is computed with the moments method, that is, from Euclidean-time moments of two-point, heavy-heavy-meson correlation functions (see also Sec. 9.8 for a description of the method).

In HPQCD 14B the b-quark mass is computed from ratios of the moments R_n of heavy current-current correlation functions, namely,

$$\left[\frac{R_n r_{n-2}}{R_{n-2} r_n}\right]^{1/2} \frac{\bar{M}_{\rm kin}}{2m_b} = \frac{\bar{M}_{\Upsilon,\eta_b}}{2\bar{m}_b(\mu)} \,, \tag{66}$$

where r_n are the perturbative moments calculated at N^{3}LO, $\bar{M}_{\rm kin}$ is the spin-averaged kinetic mass of the heavy-heavy vector and pseudoscalar mesons and $\bar{M}_{\Upsilon,\eta_b}$ is the experimental spin average of the Υ and η_b masses. The average kinetic mass $\bar{M}_{\rm kin}$ is chosen since in the lattice calculation the splitting of the Υ and η_b states is inverted. In Eq. (66), the bare mass m_b appearing on the left-hand side is tuned so that the spin-averaged mass agrees with experiment, while the mass $\overline{m}_b$ at the fixed scale $\mu = 4.18$ GeV is extrapolated to the continuum limit using three HISQ (MILC) ensembles with $a \approx 0.15$, 0.12 and 0.09 fm and two pion masses, one of which is the physical one. Their final result is $\overline{m}_b(\mu = 4.18\,\mathrm{GeV}) = 4.207(26)$ GeV, where the error is from adding systematic uncertainties in quadrature only (statistical errors are smaller than 0.1% and ignored). The errors arise from renormalization, perturbation theory, lattice spacing, and NRQCD systematics. The finite-volume uncertainty is not estimated, but at the lowest pion mass they have $m_\pi L \simeq 4$, which leads to the tag ★ .

The next four-flavour result [101] is from the ETM collaboration and updates their preliminary result appearing in a conference proceedings [103]. The calculation is performed on a set of configurations generated with twisted-Wilson fermions with three lattice spacings in the range 0.06 to 0.09 fm and with pion masses in the range 210 to 440 MeV. The b-quark mass is determined from a ratio of heavy-light pseudoscalar meson masses designed to yield the quark pole mass in the static limit. The pole mass is related to the $\overline{\rm MS}$ mass through perturbation theory at N^{3}LO. The key idea is that by taking ratios of ratios, the b-quark mass is accessible through fits to heavy-light(strange)-meson correlation functions computed on the lattice in the range ~ 1–$2 \times m_c$ and the static limit, the latter being exactly 1. By simulating below $\overline{m}_b$, taking the continuum limit is easier. They find $\overline{m}_b(\overline{m}_b) = 4.26(3)(10)$ GeV, where the first error is statistical and the second systematic. The dominant errors come from setting the lattice scale and fit systematics.

Gambino *et al.* [100] use twisted-mass-fermion ensembles from the ETM collaboration and the ETM ratio method as in ETM 16. Three values of the lattice spacing are used, ranging from 0.062 to 0.089 fm. Several volumes are also used. The light-quark masses produce pions with masses from 210 to 450 MeV. The main difference with ETM 16 is that the authors use the kinetic mass defined in the heavy-quark expansion (HQE) to extract the b-quark mass instead of the pole mass.

The final b-quark mass result is FNAL/MILC/TUM 18 [65]. The mass is extracted from the same fit and analysis done for the charm quark mass. Note that relativistic HISQ valence masses reach the physical b mass on the two finest lattice spacings ($a = 0.042$ fm, 0.03 fm) at physical and 0.2 m_s light-quark mass, respectively. In lattice units the heavy valence masses correspond to $aM^{\rm RGI} > 0.90$, making the continuum extrapolation challenging, but the authors investigated the effect of leaving out the heaviest points from the fit, and the result did not noticeably change. Their results are also consistent with an analysis dropping the finest lattice from the fit. Since the b-quark mass region is only reached with two lattice spacings, we rate this work with a green circle for the continuum extrapolation. Note however that for other values of the quark masses they use up to five values of the lattice spacing (cf. their charm-quark mass determination).

All of the above results enter our average. We note that here the ETM 16 result is consistent with the average and a stretching factor on the error is not used. The average and error is dominated by the very precise FNAL/MILC/TUM 18 value,

$$N_f = 2+1+1: \qquad \overline{m}_b(\overline{m}_b) = 4.203(11) \text{ GeV} \qquad \text{Refs. [65, 67, 99–102]}. \tag{67}$$

We have included a 100% correlation on the statistical errors of ETM 16 and Gambino 17, since the same ensembles are used in both. While FNAL/MILC/TUM 18 and HPQCD 21 also use the same MILC HISQ ensembles, the statistical error in the HPQCD 21 analysis is negligible, so we do not include a correlation between them. The average has $\chi^2/\text{dof} = 0.02$.

The above translates to the RGI average

$$N_f = 2+1+1: \qquad M_b^{\text{RGI}} = 6.934(18)_m(55)_\Lambda \text{ GeV} \qquad \text{Refs. [65, 67, 99–102]}. \tag{68}$$

All the results for $\overline{m}_b(\overline{m}_b)$ discussed above are shown in Fig. 7 together with the FLAG averages corresponding to $N_f = 2+1$ and $2+1+1$ quark flavours.

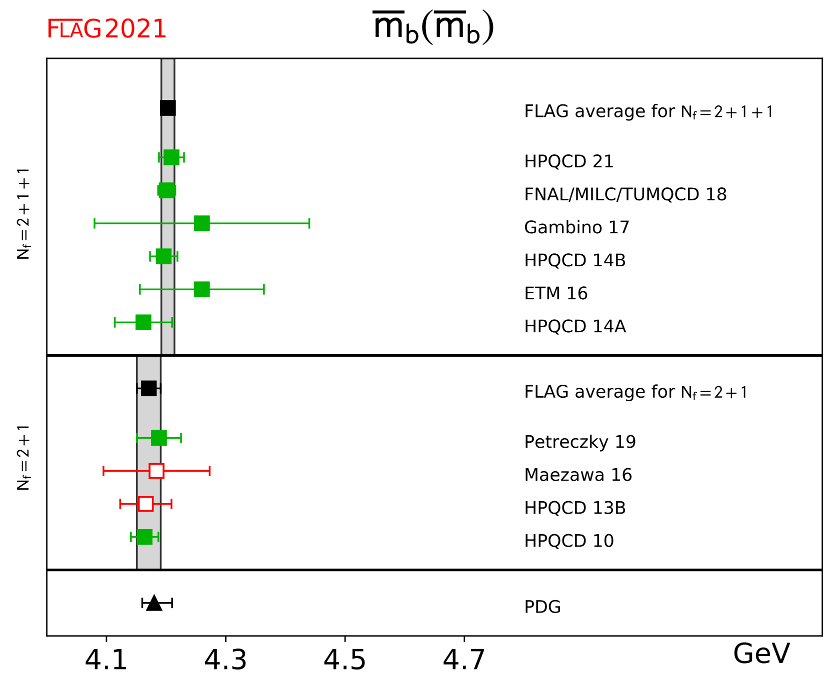

Figure 7: The b-quark mass for $N_f = 2+1$ and $2+1+1$ flavours. The updated PDG value from Ref. [1] is reported for comparison.

References

[1] Particle Data Group collaboration, *Review of Particle Physics*, PTEP **2020** (2020) 083C01.

[2] J. Gasser and H. Leutwyler, *Quark masses*, Phys. Rept. **87** (1982) 77.

[3] [ALPHA 20] R. Höllwieser, F. Knechtli and T. Korzec, *Scale setting for $N_f = 3 + 1$ QCD*, Eur. Phys. J. C **80** (2020) 349 [2002.02866].

[4] A. Athenodorou, J. Finkenrath, F. Knechtli, T. Korzec, B. Leder, M.K. Marinkovic et al., *How perturbative are heavy sea quarks?*, Nucl. Phys. **B943** (2019) 114612 [1809.03383].

[5] [ALPHA 14A] M. Bruno, J. Finkenrath, F. Knechtli, B. Leder and R. Sommer, *Effects of Heavy Sea Quarks at Low Energies*, Phys. Rev. Lett. **114** (2015) 102001 [1410.8374].

[6] [FLAG 13] S. Aoki, Y. Aoki, C. Bernard, T. Blum, G. Colangelo et al., *Review of lattice results concerning low-energy particle physics*, Eur.Phys.J. **C74** (2014) 2890 [1310.8555].

[7] M. Gell-Mann, R. J. Oakes and B. Renner, *Behavior of current divergences under SU(3)×SU(3)*, Phys. Rev. **175** (1968) 2195.

[8] [RBC 07] T. Blum, T. Doi, M. Hayakawa, T. Izubuchi and N. Yamada, *Determination of light quark masses from the electromagnetic splitting of pseudoscalar meson masses computed with two flavors of domain wall fermions*, Phys. Rev. **D76** (2007) 114508 [0708.0484].

[9] T. Blum et al., *Electromagnetic mass splittings of the low lying hadrons and quark masses from 2+1 flavor lattice QCD+QED*, Phys. Rev. **D82** (2010) 094508 [1006.1311].

[10] [FLAG 10] G. Colangelo, S. Dürr, A. Jüttner, L. Lellouch, H. Leutwyler et al., *Review of lattice results concerning low energy particle physics*, Eur.Phys.J. **C71** (2011) 1695 [1011.4408].

[11] [RM123 11] G. M. de Divitiis, P. Dimopoulos, R. Frezzotti, V. Lubicz, G. Martinelli et al., *Isospin breaking effects due to the up-down mass difference in lattice QCD*, JHEP **1204** (2012) 124 [1110.6294].

[12] [RM123 13] G. M. de Divitiis, R. Frezzotti, V. Lubicz, G. Martinelli, R. Petronzio et al., *Leading isospin breaking effects on the lattice*, Phys.Rev. **D87** (2013) 114505 [1303.4896].

[13] [RM123 17] D. Giusti, V. Lubicz, C. Tarantino, G. Martinelli, S. Sanfilippo, S. Simula et al., *Leading isospin-breaking corrections to pion, kaon and charmed-meson masses with Twisted-Mass fermions*, Phys. Rev. **D95** (2017) 114504 [1704.06561].

[14] [BMW 13A] Sz. Borsanyi et al., *Isospin splittings in the light baryon octet from lattice QCD and QED*, Phys. Rev. Lett. **111** (2013) 252001 [1306.2287].

[15] J. Bijnens and N. Danielsson, *Electromagnetic Corrections in partially quenched chiral perturbation theory*, *Phys. Rev.* **D75** (2007) 014505 [hep-lat/0610127].

[16] [BMW 16] Z. Fodor, C. Hoelbling, S. Krieg, L. Lellouch, T. Lippert, A. Portelli et al., *Up and down quark masses and corrections to Dashen's theorem from lattice QCD and quenched QED*, *Phys. Rev. Lett.* **117** (2016) 082001 [1604.07112].

[17] [BMW 20] Sz. Borsanyi et al., *Leading hadronic contribution to the muon magnetic moment from lattice QCD*, *Nature* **593** (2021) 51 [2002.12347].

[18] [BMW 14] Sz. Borsanyi et al., *Ab initio calculation of the neutron-proton mass difference*, *Science* **347** (2015) 1452 [1406.4088].

[19] [QCDSF/UKQCD 15A] R. Horsley et al., *QED effects in the pseudoscalar meson sector*, *JHEP* **04** (2016) 093 [1509.00799].

[20] [MILC 18] S. Basak et al., *Lattice computation of the electromagnetic contributions to kaon and pion masses*, *Phys. Rev.* **D99** (2019) 034503 [1807.05556].

[21] M. Hansen, B. Lucini, A. Patella and N. Tantalo, *Gauge invariant determination of charged hadron masses*, *JHEP* **05** (2018) 146 [1802.05474].

[22] B. Lucini, A. Patella, A. Ramos and N. Tantalo, *Charged hadrons in local finite-volume QED+QCD with C^* boundary conditions*, *JHEP* **02** (2016) 076 [1509.01636].

[23] A. Duncan, E. Eichten and H. Thacker, *Electromagnetic splittings and light quark masses in lattice QCD*, *Phys. Rev. Lett.* **76** (1996) 3894 [hep-lat/9602005].

[24] M. Hayakawa and S. Uno, *QED in finite volume and finite size scaling effect on electromagnetic properties of hadrons*, *Prog. Theor. Phys.* **120** (2008) 413 [0804.2044].

[25] Z. Davoudi and M.J. Savage, *Finite-Volume Electromagnetic Corrections to the Masses of Mesons, Baryons and Nuclei*, *Phys. Rev.* **D90** (2014) 054503 [1402.6741].

[26] Z. Fodor, C. Hoelbling, S.D. Katz, L. Lellouch, A. Portelli, K.K. Szabo et al., *Quantum electrodynamics in finite volume and nonrelativistic effective field theories*, *Phys. Lett.* **B755** (2016) 245 [1502.06921].

[27] N. Tantalo, V. Lubicz, G. Martinelli, C.T. Sachrajda, F. Sanfilippo and S. Simula, *Electromagnetic corrections to leptonic decay rates of charged pseudoscalar mesons: finite-volume effects*, 1612.00199.

[28] Z. Davoudi, J. Harrison, A. Jüttner, A. Portelli and M.J. Savage, *Theoretical aspects of quantum electrodynamics in a finite volume with periodic boundary conditions*, *Phys. Rev.* **D99** (2019) 034510 [1810.05923].

[29] J. Bijnens, J. Harrison, N. Hermansson-Truedsson, T. Janowski, A. Jüttner and A. Portelli, *Electromagnetic finite-size effects to the hadronic vacuum polarization*, *Phys. Rev. D* **100** (2019) 014508 [1903.10591].

[30] M. Göckeler, R. Horsley, E. Laermann, P.E.L. Rakow, G. Schierholz, R. Sommer et al., *QED: A Lattice Investigation of the Chiral Phase Transition and the Nature of the Continuum Limit*, *Nucl. Phys.* **B334** (1990) 527.

[31] M.G. Endres, A. Shindler, B.C. Tiburzi and A. Walker-Loud, *Massive photons: an infrared regularization scheme for lattice QCD+QED*, Phys. Rev. Lett. **117** (2016) 072002 [1507.08916].

[32] U.J. Wiese, *C periodic and G periodic QCD at finite temperature*, Nucl. Phys. B **375** (1992) 45.

[33] L. Polley, *Boundaries for SU(3)(C) x U(1)-el lattice gauge theory with a chemical potential*, Z. Phys. C **59** (1993) 105.

[34] P. Boyle, V. Gülpers, J. Harrison, A. Jüttner, C. Lehner, A. Portelli et al., *Isospin breaking corrections to meson masses and the hadronic vacuum polarization: a comparative study*, JHEP **09** (2017) 153 [1706.05293].

[35] [RBC/UKQCD 12] R. Arthur et al., *Domain wall QCD with near-physical pions*, Phys.Rev. **D87** (2013) 094514 [1208.4412].

[36] [ALPHA 19] M. Bruno, I. Campos, P. Fritzsch, J. Koponen, C. Pena, D. Preti et al., *Light quark masses in $N_{\rm f} = 2 + 1$ lattice QCD with Wilson fermions*, Eur. Phys. J. C **80** (2020) 169 [1911.08025].

[37] Y. Maezawa and P. Petreczky, *Quark masses and strong coupling constant in 2+1 flavor QCD*, Phys. Rev. **D94** (2016) 034507 [1606.08798].

[38] [RBC/UKQCD 14B] T. Blum et al., *Domain wall QCD with physical quark masses*, Phys. Rev. **D93** (2016) 074505 [1411.7017].

[39] [PACS-CS 12] S. Aoki, K.-I. Ishikawa, N. Ishizuka, K. Kanaya, Y. Kuramashi et al., *1+1+1 flavor QCD + QED simulation at the physical point*, Phys.Rev. **D86** (2012) 034507 [1205.2961].

[40] J. Laiho and R.S. Van de Water, *Pseudoscalar decay constants, light-quark masses and B_K from mixed-action lattice QCD*, PoS **LATTICE2011** (2011) 293 [1112.4861].

[41] [BMW 10A] S. Dürr, Z. Fodor, C. Hoelbling, S. Katz, S. Krieg et al., *Lattice QCD at the physical point: light quark masses*, Phys.Lett. **B701** (2011) 265 [1011.2403].

[42] [BMW 10B] S. Dürr, Z. Fodor, C. Hoelbling, S. Katz, S. Krieg et al., *Lattice QCD at the physical point: simulation and analysis details*, JHEP **1108** (2011) 148 [1011.2711].

[43] [PACS-CS 10] S. Aoki et al., *Non-perturbative renormalization of quark mass in $N_f = 2{+}1$ QCD with the Schrödinger functional scheme*, JHEP **1008** (2010) 101 [1006.1164].

[44] [MILC 10A] A. Bazavov et al., *Staggered chiral perturbation theory in the two-flavor case and SU(2) analysis of the MILC data*, PoS **LAT2010** (2010) 083 [1011.1792].

[45] [HPQCD 10] C. McNeile, C. T. H. Davies, E. Follana, K. Hornbostel and G. P. Lepage, *High-precision c and b masses and QCD coupling from current-current correlators in lattice and continuum QCD*, Phys. Rev. **D82** (2010) 034512 [1004.4285].

[46] [RBC/UKQCD 10A] Y. Aoki et al., *Continuum limit physics from 2+1 flavor domain wall QCD*, Phys.Rev. **D83** (2011) 074508 [1011.0892].

[47] [PACS-CS 09] S. Aoki et al., *Physical point simulation in 2+1 flavor lattice QCD*, *Phys. Rev.* **D81** (2010) 074503 [0911.2561].

[48] [HPQCD 09A] C. T. H. Davies et al., *Precise charm to strange mass ratio and light quark masses from full lattice QCD*, *Phys. Rev. Lett.* **104** (2010) 132003 [0910.3102].

[49] [MILC 09A] A. Bazavov et al., *MILC results for light pseudoscalars*, *PoS* **CD09** (2009) 007 [0910.2966].

[50] [MILC 09] A. Bazavov et al., *Full nonperturbative QCD simulations with 2+1 flavors of improved staggered quarks*, *Rev. Mod. Phys.* **82** (2010) 1349 [0903.3598].

[51] [PACS-CS 08] S. Aoki et al., *2+1 flavor lattice QCD toward the physical point*, *Phys. Rev.* **D79** (2009) 034503 [0807.1661].

[52] [RBC/UKQCD 08] C. Allton et al., *Physical results from 2+1 flavor domain wall QCD and SU(2) chiral perturbation theory*, *Phys. Rev.* **D78** (2008) 114509 [0804.0473].

[53] [CP-PACS/JLQCD 07] T. Ishikawa et al., *Light quark masses from unquenched lattice QCD*, *Phys. Rev.* **D78** (2008) 011502 [0704.1937].

[54] [HPQCD 05] Q. Mason, H. D. Trottier, R. Horgan, C. T. H. Davies and G. P. Lepage, *High-precision determination of the light-quark masses from realistic lattice QCD*, *Phys. Rev.* **D73** (2006) 114501 [hep-ph/0511160].

[55] [MILC 04] C. Aubin et al., *Light pseudoscalar decay constants, quark masses and low energy constants from three-flavor lattice QCD*, *Phys. Rev.* **D70** (2004) 114501 [hep-lat/0407028].

[56] [HPQCD/MILC/UKQCD 04] C. Aubin et al., *First determination of the strange and light quark masses from full lattice QCD*, *Phys. Rev.* **D70** (2004) 031504 [hep-lat/0405022].

[57] T. van Ritbergen, J. A. M. Vermaseren and S. A. Larin, *The four-loop β-function in Quantum Chromodynamics*, *Phys. Lett.* **B400** (1997) 379 [hep-ph/9701390].

[58] K.G. Chetyrkin and A. Retey, *Renormalization and running of quark mass and field in the regularization invariant and $\overline{\rm MS}$ schemes at three and four loops*, *Nucl. Phys.* **B583** (2000) 3 [hep-ph/9910332].

[59] Particle Data Group collaboration, *Review of Particle Physics*, *Chin. Phys.* **C38** (2014) 090001 and 2015 update.

[60] [HPQCD 08B] I. Allison et al., *High-precision charm-quark mass from current-current correlators in lattice and continuum QCD*, *Phys. Rev.* **D78** (2008) 054513 [0805.2999].

[61] M. Bruno et al., *Simulation of QCD with $N_f = 2 + 1$ flavors of non-perturbatively improved Wilson fermions*, *JHEP* **02** (2015) 043 [1411.3982].

[62] [ALPHA 18C] I. Campos, P. Fritzsch, C. Pena, D. Preti, A. Ramos and A. Vladikas, *Non-perturbative quark mass renormalisation and running in $N_f = 3$ QCD*, *Eur. Phys. J. C* **78** (2018) 387 [1802.05243].

[63] [ETM 21A] C. Alexandrou et al., *Quark masses using twisted mass fermion gauge ensembles*, *Phys. Rev. D* **104** (2021) 074515 [2104.13408].

[64] [ETM 14] N. Carrasco et al., *Up, down, strange and charm quark masses with N_f = 2+1+1 twisted mass lattice QCD*, *Nucl. Phys.* **B887** (2014) 19 [1403.4504].

[65] [FNAL/MILC/TUMQCD 18] A. Bazavov et al., *Up-, down-, strange-, charm-, and bottom-quark masses from four-flavor lattice QCD*, *Phys. Rev.* **D98** (2018) 054517 [1802.04248].

[66] [HPQCD 18] A. T. Lytle, C.T.H. Davies, D. Hatton, G.P. Lepage and C. Sturm, *Determination of quark masses from $\mathbf{n_f = 4}$ lattice QCD and the RI-SMOM intermediate scheme*, *Phys. Rev.* **D98** (2018) 014513 [1805.06225].

[67] [HPQCD 14A] B. Chakraborty, C.T.H. Davies, G.C. Donald, R.J. Dowdall, B. Galloway, P. Knecht et al., *High-precision quark masses and QCD coupling from $n_f = 4$ lattice QCD*, *Phys.Rev.* **D91** (2015) 054508 [1408.4169].

[68] C.A. Dominguez, N.F. Nasrallah, R. Röntsch and K. Schilcher, *Light quark masses from QCD sum rules with minimal hadronic bias*, *Nucl. Phys. Proc. Suppl.* **186** (2009) 133 [0808.3909].

[69] K.G. Chetyrkin and A. Khodjamirian, *Strange quark mass from pseudoscalar sum rule with $O(\alpha_s^4)$ accuracy*, *Eur. Phys. J.* **C46** (2006) 721 [hep-ph/0512295].

[70] M. Jamin, J.A. Oller and A. Pich, *Scalar $K\pi$ form factor and light quark masses*, *Phys. Rev.* **D74** (2006) 074009 [hep-ph/0605095].

[71] S. Narison, *Strange quark mass from e^+e^- revisited and present status of light quark masses*, *Phys. Rev.* **D74** (2006) 034013 [hep-ph/0510108].

[72] A.I. Vainshtein et al., *Sum rules for light quarks in Quantum Chromodynamics*, *Sov. J. Nucl. Phys.* **27** (1978) 274.

[73] K. Maltman and J. Kambor, *$m_u + m_d$ from isovector pseudoscalar sum rules*, *Phys. Lett.* **B517** (2001) 332 [hep-ph/0107060].

[74] [FNAL/MILC 17] A. Bazavov et al., *B- and D-meson leptonic decay constants from four-flavor lattice QCD*, *Phys. Rev.* **D98** (2018) 074512 [1712.09262].

[75] [FNAL/MILC 14A] A. Bazavov et al., *Charmed and light pseudoscalar meson decay constants from four-flavor lattice QCD with physical light quarks*, *Phys.Rev.* **D90** (2014) 074509 [1407.3772].

[76] [FLAG 19] S. Aoki et al., *FLAG Review 2019: Flavour Lattice Averaging Group (FLAG)*, *Eur. Phys. J. C* **80** (2020) 113 [1902.08191].

[77] J.A. Oller and L. Roca, *Non-perturbative study of the light pseudoscalar masses in chiral dynamics*, *Eur. Phys. J.* **A34** (2007) 371 [hep-ph/0608290].

[78] R. Kaiser, *The η and the η' at large N_c, diploma work, University of Bern* (1997); H. Leutwyler, *On the 1/N-expansion in chiral perturbation theory*, *Nucl. Phys. Proc. Suppl.* **64** (1998) 223 [hep-ph/9709408].

[79] H. Leutwyler, *The ratios of the light quark masses*, *Phys. Lett.* **B378** (1996) 313 [hep-ph/9602366].

[80] S. Weinberg, *The problem of mass*, *Trans. New York Acad. Sci.* **38** (1977) 185.

[81] R.F. Dashen, *Chiral SU(3)×SU(3) as a symmetry of the strong interactions*, *Phys. Rev.* **183** (1969) 1245.

[82] A. Portelli, *Inclusion of isospin breaking effects in lattice simulations*, *PoS* **LATTICE2014** (2015) 013.

[83] [ETM 10] R. Baron et al., *Light hadrons from lattice QCD with light (u,d), strange and charm dynamical quarks*, *JHEP* **1006** (2010) 111 [1004.5284].

[84] [MILC 16] S. Basak et al., *Electromagnetic effects on the light pseudoscalar mesons and determination of m_u/m_d*, *PoS* **LATTICE2015** (2016) 259 [1606.01228].

[85] H. Leutwyler, *Light quark masses*, *PoS* **CD09** (2009) 005 [0911.1416].

[86] [QCDSF/UKQCD 15] R. Horsley et al., *Isospin splittings of meson and baryon masses from three-flavor lattice QCD + QED*, *J. Phys.* **G43** (2016) 10LT02 [1508.06401].

[87] [ALPHA 05] M. Della Morte et al., *Non-perturbative quark mass renormalization in two-flavor QCD*, *Nucl. Phys.* **B729** (2005) 117 [hep-lat/0507035].

[88] [BMW 12] A. Portelli, S. Dürr, Z. Fodor, J. Frison, C. Hoelbling et al., *Systematic errors in partially-quenched QCD plus QED lattice simulations*, *PoS* **LAT2011** (2011) 136 [1201.2787].

[89] J. Gasser and H. Leutwyler, *$\eta \to 3\pi$ to one loop*, *Nucl. Phys.* **B250** (1985) 539.

[90] G. Colangelo, S. Lanz, H. Leutwyler and E. Passemar, *Dispersive analysis of $\eta \to 3\pi$*, *Eur. Phys. J.* **C78** (2018) 947 [1807.11937].

[91] G. Amoros, J. Bijnens and P. Talavera, *QCD isospin breaking in meson masses, decay constants and quark mass ratios*, *Nucl. Phys.* **B602** (2001) 87 [hep-ph/0101127].

[92] [FLAG 16] S. Aoki et al., *Review of lattice results concerning low-energy particle physics*, *Eur. Phys. J.* **C77** (2017) 112 [1607.00299].

[93] [HPQCD 20A] D. Hatton, C.T.H. Davies, B. Galloway, J. Koponen, G.P. Lepage and A.T. Lytle, *Charmonium properties from lattice QCD+QED : Hyperfine splitting, J/ψ leptonic width, charm quark mass, and a_μ^c*, *Phys. Rev. D* **102** (2020) 054511 [2005.01845].

[94] [ETM 14A] C. Alexandrou, V. Drach, K. Jansen, C. Kallidonis and G. Koutsou, *Baryon spectrum with $N_f = 2+1+1$ twisted mass fermions*, *Phys. Rev.* **D90** (2014) 074501 [1406.4310].

[95] [ALPHA 21] J. Heitger, F. Joswig and S. Kuberski, *Determination of the charm quark mass in lattice QCD with $2+1$ flavours on fine lattices*, *JHEP* **05** (2021) 288 [2101.02694].

[96] P. Petreczky and J. Weber, *Strong coupling constant and heavy quark masses in (2+1)-flavor QCD*, *Phys. Rev. D* **100** (2019) 034519 [1901.06424].

[97] [JLQCD 16] K. Nakayama, B. Fahy and S. Hashimoto, *Short-distance charmonium correlator on the lattice with Möbius domain-wall fermion and a determination of charm quark mass*, *Phys. Rev.* **D94** (2016) 054507 [1606.01002].

[98] [χQCD 14] Y. Yi-Bo et al., *Charm and strange quark masses and f_D_s from overlap fermions*, *Phys. Rev.* **D92** (2015) 034517 [1410.3343].

[99] [HPQCD 21] D. Hatton, C.T.H. Davies, J. Koponen, G.P. Lepage and A.T. Lytle, *Determination of $\overline{m}_b/\overline{m}_c$ and $\overline{m}_b$ from $n_f = 4$ lattice QCD+QED*, *Phys. Rev. D* **103** (2021) 114508 [2102.09609].

[100] P. Gambino, A. Melis and S. Simula, *Extraction of heavy-quark-expansion parameters from unquenched lattice data on pseudoscalar and vector heavy-light meson masses*, *Phys. Rev.* **D96** (2017) 014511 [1704.06105].

[101] [ETM 16B] A. Bussone et al., *Mass of the b quark and B -meson decay constants from N_f=2+1+1 twisted-mass lattice QCD*, *Phys. Rev.* **D93** (2016) 114505 [1603.04306].

[102] [HPQCD 14B] B. Colquhoun, R.J. Dowdall, C.T.H. Davies, K. Hornbostel and G.P. Lepage, *Υ and Υ' Leptonic Widths, a_μ^b and m_b from full lattice QCD*, *Phys. Rev.* **D91** (2015) 074514 [1408.5768].

[103] [ETM 14B] A. Bussone et al., *Heavy flavour precision physics from $N_f = 2+1+1$ lattice simulations*, in *International Conference on High Energy Physics 2014 (ICHEP 2014) Valencia, Spain, July 2-9, 2014*, vol. 273-275, pp. 273–275, 2016, DOI [1411.0484].

[104] [HPQCD 13B] A.J. Lee et al., *Mass of the b quark from lattice NRQCD and lattice perturbation theory*, *Phys. Rev.* **D87** (2013) 074018 [1302.3739].

[105] [ETM 13B] N. Carrasco et al., *B-physics from $N_f = 2$ tmQCD: the Standard Model and beyond*, *JHEP* **1403** (2014) 016 [1308.1851].

[106] [ALPHA 13C] F. Bernardoni et al., *The b-quark mass from non-perturbative $N_f = 2$ Heavy Quark Effective Theory at $O(1/m_h)$*, *Phys. Lett.* **B730** (2014) 171 [1311.5498].

[107] [ETM 11A] P. Dimopoulos et al., *Lattice QCD determination of m_b, f_B and f_{B_s} with twisted mass Wilson fermions*, *JHEP* **1201** (2012) 046 [1107.1441].